



**AN INVESTIGATION OF THE EFFECTS OF BOUNDARY AVOIDANCE ON
PILOT TRACKING**

THESIS

Randy D. Warren, Captain, USAF

AFIT/GAE/ENY/06-S11

**DEPARTMENT OF THE AIR FORCE
AIR UNIVERSITY**

AIR FORCE INSTITUTE OF TECHNOLOGY

Wright-Patterson Air Force Base, Ohio

APPROVED FOR PUBLIC RELEASE; DISTRIBUTION UNLIMITED

The views expressed in this thesis are those of the author and do not reflect the official policy or position of the United States Air Force, Department of Defense, or the U.S. Government.

AFIT/GAE/ENY/06-S11

**AN INVESTIGATION OF THE EFFECTS OF BOUNDARY AVOIDANCE ON
PILOT TRACKING**

THESIS

Presented to the Faculty

Department of Aeronautics and Astronautics

Graduate School of Engineering and Management

Air Force Institute of Technology

Air University

Air Education and Training Command

In Partial Fulfillment of the Requirements for the
Degree of Master of Science in Aeronautical Engineering

Randy D. Warren, BS

Captain, USAF

September 2006

APPROVED FOR PUBLIC RELEASE; DISTRIBUTION UNLIMITED

Abstract

Pilot-Involved Oscillations (PIOs) remain a significant issue in the design, testing and operations of aerospace vehicles. Traditional methods for predicting, describing, and analyzing these events have provided the community with improved methods for minimizing the occurrences of PIOs. However, these events continue to occur over a wide range of aerospace vehicle types and over a wide range of pilot acumen.

The introduction of boundary avoidance tracking (BAT) by Mr. William Gray in 2004 added a missing piece to the PIO puzzle. This theory presented that PIOs may result from increasing pilot gain resulting not from maintaining a specified condition, but avoiding imposed limits or boundaries on a specified task. The initial modeling and simulation conducted by Mr. Gray has provided the community with a starting point for applying this theory to the analysis of PIO events.

This thesis characterizes BAT in the dynamic flight environment. Through the analysis of repeated BAT events in a T-38C aircraft, initial characteristic parameters for BAT have been identified and developed. The key BAT parameters were found to be independent of pilot and exhibited some dependence on aircraft load factor. Overall, BAT was successfully demonstrated and characterized during this research and the results will provide the community with a better understanding of the role BAT plays in PIO prediction and analysis.

Acknowledgments

I would like to start by thanking my thesis advisor, Maj. Paul Blue, for his continual coaching and support during this endeavor. Thanks for sticking with me and by me for the duration of this project.

I owe a great deal of gratitude to Mr. Bill Gray for allowing me to be a part of his developing field of research and study. Thank you for the many hours of patience in working with me and for your guidance and support during the development and execution of this research.

To my test team at the Air Force Test Pilot School – Maj. Scott Heritsch, Maj. Brian Abell, Capt. Kyle Kolsti, and Capt. Brandon Miller – thanks for your hours of dedication to this research project. Your help, friendship, and professionalism made this project a success and I'm forever grateful for your support. Thanks to Lt. Jay Kemper for his tireless effort to develop, test, and operate a fully functional T-38 simulator.

Thanks to my wife and son for their years of support and understanding along this long road. You stuck by all along and there is no way I could have finished this without you. I'm forever grateful and humbled by your love and dedication.

Finally, I am eternally indebted to Jesus Christ for his carrying me along the way. His love and devotion to me could never be reciprocated by my human heart. I will spend the rest of my days trying to live up to the standard you have set. Through your love and grace all things were possible during this time and they will forever continue to be.

Table of Contents

	Page
Abstract.....	iv
Acknowledgments.....	v
Table of Contents.....	vi
List of Figures.....	x
List of Tables.....	xii
List of Abbreviations, Symbols, and Acronyms.....	xiii
1. Introduction.....	1
1.1 Motivation.....	1
1.2 Tracking Tasks.....	2
1.2.1 Point Tracking.....	2
1.2.2 Boundary Avoidance Tracking.....	3
1.2.3 Comparison of Point Tracking and Boundary Avoidance Tracking.....	4
1.3 Research Objectives.....	4
1.4 Experiment Overview.....	5
1.5 Preview of Results.....	5
1.6 Thesis Overview.....	6
2. Background.....	7
2.1 Boundary Avoidance Tracking Introduction.....	7
2.1.1 Point Tracking.....	7
2.1.2 Boundary Avoidance Tracking.....	8
2.2 Modeling Boundary Avoidance Tracking.....	9
2.2.1 Model Assumptions.....	10

2.2.2	Point Tracking Pilot Model.....	13
2.2.3	Boundary Tracking Pilot Model	13
2.2.4	System Plant.....	14
2.2.5	Model Results	14
2.2.6	Boundary Avoidance Tracking Modeling Summary	19
2.3	Simulating Boundary Avoidance Tracking	20
2.3.1	Simulator Tracking Task.....	20
2.3.2	Simulator Data Reduction.....	22
2.3.3	Simulator Results	22
3.	Research Objectives and Experiment Methodology	24
3.1	Research Overview.....	24
3.1.1	System Definition	24
3.1.2	Boundary Avoidance Tracking Parameters	25
3.1.3	Aircraft Flying Qualities	26
3.2	Experiment Design	27
3.2.1	Pilot Tracking Task.....	28
3.2.2	Pilot Mindset.....	29
3.2.3	Flight Conditions	29
3.3	Fixed-Base Simulation	30
3.3.1	Simulator Properties.....	30
3.3.2	Aircraft Flying Qualities Flight Test Technique Development	33
3.3.3	Boundary Avoidance Tracking Flight Test Technique Development	34

3.4	Experiment Instrumentation	36
3.4.1	Aircraft Visual Markings	37
3.4.2	Aircraft Mounted Camera System	38
3.4.3	Aircraft Data Acquisition System.....	40
4.	Analysis and Results	41
4.1	Research Assumptions.....	41
4.1.1	Aircraft Mounted Camera	41
4.1.2	Vertical Motion Constraint	41
4.2	Data Reduction Algorithms	42
4.2.1	Automated Visual Tracking Routine	44
4.2.2	Manual Visual Data Reduction Routine	46
4.2.3	Aircraft Data Acquisition System Routine	47
4.3	Aircraft Flying Qualities Parameter Analysis.....	48
4.3.1	Determination of System Time Delay	48
4.3.2	Determination of System Crossover Frequency	49
4.4	Boundary Avoidance Tracking Characterization	51
4.4.1	BAT Data Analysis Tool	51
4.4.2	Estimating Longitudinal Stick Trim Position	58
4.4.3	Identification of K_{max} and t_{Kmax}	61
4.4.4	Determination of t_{Kmin}	63
4.4.5	Pilot Actuation Frequency Determination	65
4.4.6	Analysis of BAT Parameters	67

4.5 Correlation of Flying Qualities and Boundary Avoidance Tracking	77
4.6 Aircrew Comments.....	79
4.6.1 Flying Qualities Effects	79
4.6.2 PIOs Resulting From Repeated Boundary Avoidance Tracking Events	80
5. Discussion.....	81
5.1 Summary of Findings	81
5.2 Lessons Learned	82
5.3 Recommendations for Future Research.....	82
Appendix – Collected Data.....	84
Bibliography	86
Vita	87

List of Figures

	Page
Figure 1. Tracking Task Illustration	3
Figure 2. Diagram of Original Boundary Avoidance Tracking Model	9
Figure 3. Boundary Tracking Model Result - Point Tracking	16
Figure 4. Boundary Tracking Model Result – Boundary Awareness	17
Figure 5. Boundary Tracking Model Result - Boundary Avoidance Tracking	19
Figure 6. Gray Simulator Tracking Task Display	21
Figure 7. Boundary Tracking Parameter (BTP) Results (Gray, 2005:11)	23
Figure 8. Tracking Task Visual Reference	28
Figure 9. AFRL Simulator Visual Presentation (Left Panel Display)	32
Figure 10. Target Aircraft Visual Markings	37
Figure 11. Aircraft Mounted Camera Placement	39
Figure 12. Data Reduction Flow Chart	43
Figure 13. Chromatic Filtering of Visual Data	45
Figure 14. Example ScratchClick Interface for Visual Data Extraction	47
Figure 15. BAT Data Analysis Tool – BAT_Calc	52
Figure 16. Schematic of Visual Data Point Selection	53
Figure 17. Distance to Boundary Time History – BAT_Calc Display	56
Figure 18. Time to Boundary Time History – BAT_Calc Display	58
Figure 19. Longitudinal Stick Trim Position - BAT_Calc Display	60
Figure 20. Determination of K_{max} and t_{Kmax} - Bat_Calc Display	62

Figure 21. Determination of t_{Kmin} - BAT_Calc Display.....	64
Figure 22. PSD of Longitudinal Stick Position - BAT_Calc Display	67
Figure 23. Correlation of t_{Kmin} and G_{Kmin}	70
Figure 24. Correlation of Normalized t_{Kmin} and G_{Kmin}	71
Figure 25. Correlation of G_{Kmin}/t_{Kmin} with System Crossover Frequency	78

List of Tables

	Page
Table 1. Boundary Tracking Model Parameter Values	14
Table 2. Summary of Flight Conditions	30
Table 3. Summary of Developed Flight Test Techniques	36
Table 4. System Time Delays	49
Table 5. System Crossover Frequencies	50
Table 6. Results of Statistical Analyses for t_{Kmin}	68
Table 7. Statistical Analyses of the Ratio of G_{Kmin} to t_{Kmin}	73
Table 8. Statistical Analyses of t_{Kmax}	75
Table 9. Statistical Analyses of Boundary Feedback Gain.....	75

List of Abbreviations, Symbols, and Acronyms

<u>Symbol</u>	<u>Definition</u>	<u>Units</u>
Δt	Time between minimum and maximum gains	sec
$(\Delta G/\Delta t)_{K_{max}}$	Time rate of change of load factor at maximum gain	G/sec
$(\Delta G/\Delta t)_{K_{min}}$	Time rate of change of load factor at minimum gain	G/sec
τ_b	Boundary tracking time delay	sec
τ_{delay}	System time delay	sec
τ_{PT}	Pilot time delay during point tracking task	sec
ω_{180}	System crossover frequency	Hz
ω_{BAT}	Pilot actuation frequency	Hz
D_{lower}	Distance to lower boundary	pix
D_{upper}	Distance to upper boundary	pix
$G_{K_{max}}$	Load factor at maximum gain	G
$G_{K_{min}}$	Load factor at minimum gain	G
h_{b-1}	Boundary distance for Example 1 (Point Tracking)	--
h_{b-2}	Boundary distance for Example 2 (Boundary Awareness)	--
h_{b-3}	Boundary distance for Example 3 (Boundary Avoidance)	--
$K_{boundary}$	Boundary tracking feedback gain	--
K_{max}	Maximum boundary tracking feedback gain	--
K_{PT}	Point tracking feedback gain	--

<u>Symbol</u>	<u>Definition</u>	<u>Units</u>
$K_{PT-LIMIT}$	Point tracking feedback gain saturation limit	--
m_{lower}	Slope of lower boundary line	pix/pix
m_{upper}	Slope of upper boundary line	pix/pix
$r_{boundary}$	Rate to boundary	pix/sec
$t_{boundary}$	Time to boundary	sec
t_{Kmax}	Time to boundary for maximum feedback gain	sec
t_{Kmin}	Time to boundary for minimum feedback gain	sec
$x_{boundary}$	Distance to boundary	--
$\dot{x}_{boundary}$	Time rate of change of distance to boundary	--
y_{lb}	Distance between lower boundary and reference	pix
y_{lower}	Distance between wingtip and lower boundary	pix
y_{ub}	Distance between upper boundary and reference	pix
y_{upper}	Distance between wingtip and upper boundary	pix
$y_{wingtip}$	Distance between wingtip and reference	pix
ADA	Computer programming language	--
AFRL	Air Force Research Laboratory	--
AFRL/VA	AFRL Air Vehicles Directorate	--
ASC	Aeronautical Systems Center	--
AVI	Audio Video Interleave Video File Format	--
BAT	Boundary Avoidance Tracking	--
BTP	Boundary Tracking Parameter	--

<u>Symbol</u>	<u>Definition</u>	<u>Units</u>
DAS	Data Acquisition System	--
DoD	Department of Defense	--
FFT	Fast Fourier Transform	--
FOV	Field of View	--
GUI	Graphical User Interface	--
HUD	Heads-Up Display	--
IEEE	Institute of Electrical and Electronics Engineers	--
MAVE	Moving Point Average	--
MFD	Multi-Function Display	--
PIO	Pilot-Involved Oscillation	--
PSD	Power Spectral Density	--

AN INVESTIGATION OF THE EFFECTS OF BOUNDARY AVOIDANCE ON PILOT TRACKING

1. Introduction

1.1 Motivation

Pilot-Involved Oscillations (PIOs) continue to present significant problems to the aviation community. Since the advent of powered flight, pilots have reported undesirable aircraft oscillatory behavior. In fact, as aircraft have grown in complexity, so too have the variety, complexity and frequency of PIOs (McRuer, 1995:3). The continued need to develop the understanding and characterization of this handling qualities problem has been made very apparent with several high-profile PIO events.

The YF-22 suffered a destructive PIO in 1992 during an approach to a go-around; two JAS-39 Gripen aircraft were lost to PIOs during approaches in 1990 and 1993 (McRuer, 1995:9); and the C-17A experienced several PIOs during Dutch roll testing, aerial-refueling tracking, and three-engine approaches and landings (Preston and others, 1996:20-49).

Currently, modeling and testing for PIO requires a pilot to perform some sort of specified task in order to close the pilot plus aircraft loop and evaluate the system handling qualities. For example, the tasks could include aerial refueling, formation flight, precision approaches to spot landings, or many others (McRuer, 1995:4). During both modeling and testing, the pilot must minimize the error associated with the task; however, this error is not the only thing the pilot is tracking. Every task will also have

associated boundaries or limits. Whether these boundaries are placed on the task itself or are a function of the pilot or aircraft, they are a part of the scenario. Until now, these boundaries have largely been ignored in the prediction and analysis of task performance and PIO susceptibility.

1.2 Tracking Tasks

As previously stated, handling qualities are evaluated utilizing some specified task. That task has a desired condition that must be maintained and also some set of boundaries. Figure 1 illustrates an arbitrary tracking task. The figure depicts an illustration of an aircraft Heads-Up Display (HUD) set in a ground attack mode. The center circle with a dot in the middle represents the aircraft's flight path vector. The circle at the bottom connected to a line represents the impact point if a bomb was released at that moment.

1.2.1 Point Tracking

The specified task for this illustration is for the pilot to hit the designated target area. To do so, the pilot must maneuver the aircraft such that the bottom circle lines up over the designated target area. This is called the point tracking task.

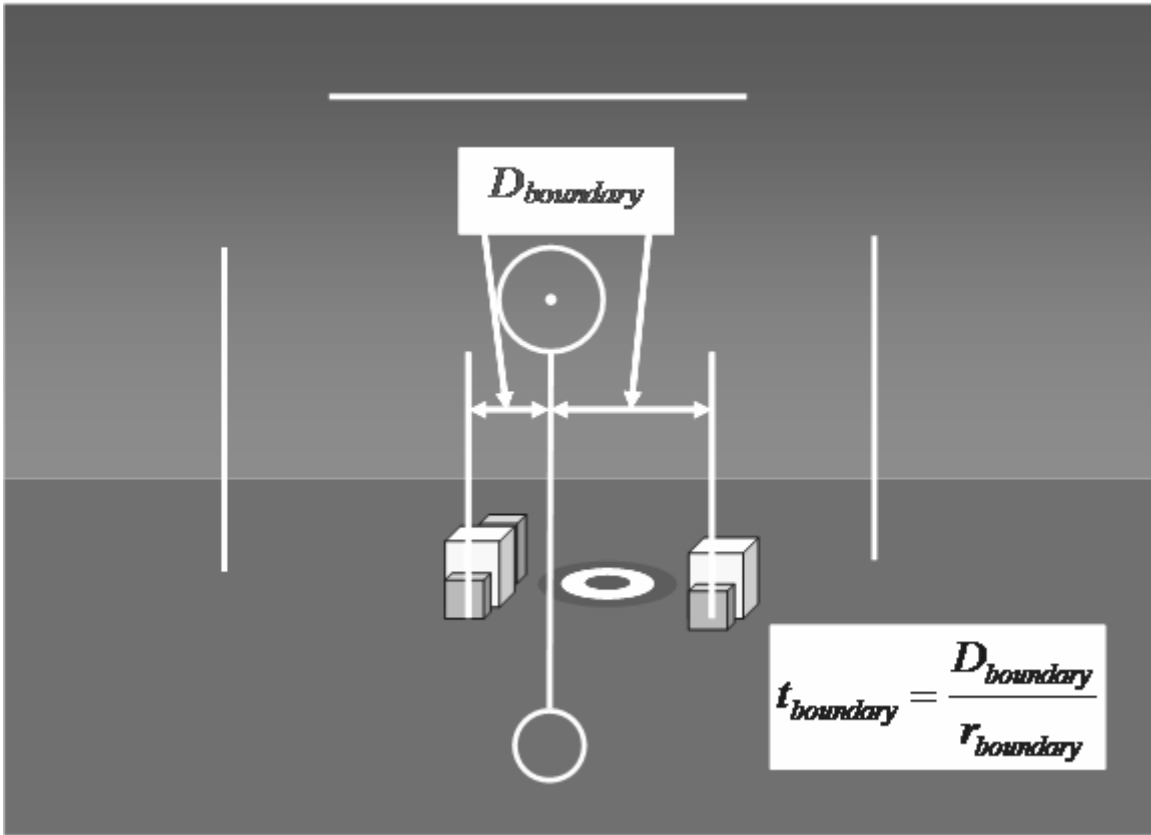


Figure 1. Tracking Task Illustration

1.2.2 Boundary Avoidance Tracking

The boundaries imposed on this task are the buildings located on each side of the designated target area. The pilot must not release his weapon onto either of these structures. As the pilot begins to approach one of these boundaries, the aircraft will be controlled away from the boundary to avoid hitting that boundary. This is called boundary avoidance tracking (BAT). The pilot is still performing the point tracking task, but inputs to the system are made to avoid a perceived approach to a boundary, not to minimize the error associated with the designated target area.

For BAT, two parameters are used to define the pilot's awareness of the boundary. First is distance to boundary, $D_{boundary}$. This is the distance the pilot perceives before a boundary is crossed (Figure 1). Second is the time to boundary, $t_{boundary}$. This time is determined from the distance to boundary and the time rate of change of the distance to boundary, $r_{boundary}$. It is believed that the primary mechanism for boundary awareness and avoidance is the pilot's perceived time to boundary. This will be discussed further in Chapter 2.

1.2.3 Comparison of Point Tracking and Boundary Avoidance Tracking

Though these two types of tracking seem somewhat similar, they are in essence the reverse of each other. With point tracking, pilots tend to decrease their level of inputs as they approach the specified condition and increase as they depart the condition. In BAT, they increase their level of inputs to avoid a boundary and decrease their inputs when departing the boundary.

As such, it is critical to understanding the boundaries levied on any given task. Since all tasks are bounded by mission, operational, structural, and aerodynamic limits, it is critical to understand how close to these boundaries a pilot may have to operate for the specified task.

1.3 Research Objectives

The focus of this research was to investigate the effect that BAT has on the ability of a pilot to accomplish a specified task. To determine this effect, BAT was characterized in a dynamic flight environment. Once it was adequately characterized, the relationship between BAT and aircraft flying qualities could be investigated.

Development of this relationship will lead to a better understanding of how BAT and aircraft flying qualities work together to affect the ability of the pilot to successfully accomplish a specified task.

1.4 Experiment Overview

BAT data were collected in the flight environment by flying two T-38 aircraft in formation with the test pilot maintaining a specified condition. The task was then bounded and the test pilot was to continue to maintain the specified condition while avoiding the boundaries. Data were collected using both an aircraft data acquisition system and a video camera system. Aircraft configuration and flight conditions were varied to present as wide a range as possible of aircraft flying qualities and multiple techniques to elicit BAT were developed and employed.

1.5 Preview of Results

While no definitive correlation between aircraft flying qualities and the BAT parameters was found, the data obtained led to further characterization of human perception and reaction to boundaries. Two parameters were identified as apparent ingrained human characteristics – the time to boundary for maximum BAT feedback gain and the time elapsed between minimum and maximum feedback gain. The time to boundary for minimum BAT feedback gain was found to be a function of aircraft load factor. Frequency domain analysis also revealed that pilots operated with very little phase margin during BAT events leading to pilot-involved oscillations (PIOs).

1.6 Thesis Overview

In Chapter 2, a detailed review of the previous work conducted by Mr. William Gray is provided. The foundation for the BAT theory developed through his modeling and simulation work are key to understanding the experiment methodology and results of this thesis. Chapter 3 details the experiment methodology and instrumentation utilized to obtain the data during the research. Chapter 4 presents the data reduction and analysis and Chapter 5 summarizes the results, lessons learned, and recommendations.

2. Background

2.1 Boundary Avoidance Tracking Introduction

The concept of BAT was first introduced by Mr. William Gray of the United States Air Force Test Pilot School to the Society of Experimental Test Pilots in 2004 (Gray, 2004:3). In his paper, Mr. Gray proposed a mechanism for PIOs that was markedly different from the traditional PIO assumptions that have governed the prediction and prevention of PIOs over the past several decades (McRuer, 1995:14-34). That is, some PIOs may be explained by the pilot successively controlling the aircraft to avoid opposing boundaries as opposed to over-controlling while point tracking.

The United States Department of Defense (DoD) defines PIO as “sustained or uncontrollable oscillations resulting from the efforts of the pilot to control the aircraft” (MIL-HDBK-1797, 1997:151). Of note is that Mr. Gray’s theory does not contradict this definition. In fact, the resulting oscillatory motion from repeated BAT events meets this definition of a PIO. This means that past PIOs may have exhibited BAT characteristics but have been unsuccessfully analyzed because point tracking techniques have been applied.

2.1.1 Point Tracking

In traditional pilot-aircraft system analysis, a point tracking task is specified and the pilot is required to maintain that condition. The pilot will provide system inputs when a tracking error is perceived in an effort to return the system to the specified condition. The pilot’s experience level, the difficulty of the task, and the aircraft’s handling qualities

(among many other factors) are all responsible for the pilot's overall performance in maintaining the specified condition.

Undesirable aircraft oscillatory motion is generally excited by the level of pilot input into the aircraft system. Through increasingly stringent levels of tracking error, the pilot is driven to a state of zero tracking error in an effort to maintain the specified condition. As this state is approached, pilot inputs increase in frequency and in some cases in amplitude as well. Once the zero error state is reached and the pilot is tracking aggressively and assiduously, the system experiences the highest frequency and amplitude inputs. It is at this state that any undesirable aircraft tendencies are generally identified (Brown, 2002:23-1).

2.1.2 Boundary Avoidance Tracking

For BAT, the pilot is no longer providing system inputs to maintain a specified condition, but is instead providing inputs in an attempt to avoid an approaching boundary. At some point, the pilot becomes aware of the boundary and begins making system inputs in an effort to stop encroaching on the boundary. At this point, the pilot has abandoned tracking the specified condition and is now attempting to avoid the approaching boundary.

If the pilot perceives that the boundary is successfully avoided, then he returns to tracking the specified condition. If the pilot perceives a continued approach to the boundary, then the level of pilot input increases. As the approach to the boundary becomes more rapid, the magnitude of pilot input to avoid that boundary also increases.

Since this type of tracking only occurs with pilot awareness of the imposed boundaries, BAT is transient in nature. If the boundaries are sufficiently wide as to allow a large envelope of motion, it is quite possible that a pilot may never engage in a BAT event during a specific task. However, as the boundaries become tighter, the pilot-aircraft system can become unstable and result in PIOs.

2.2 Modeling Boundary Avoidance Tracking

In an effort to better understand, explain, and characterize BAT, Mr. Gray created the first BAT model (Gray, 2004:11). The system, shown in Figure 2, was composed of a simple pilot model and a second order system with rate and displacement as the primary feedback mechanisms. The feedback loop was composed of both point and boundary tracking algorithms with a logic switch that forced the system to select between application of point tracking feedback gains or boundary tracking feedback gains.

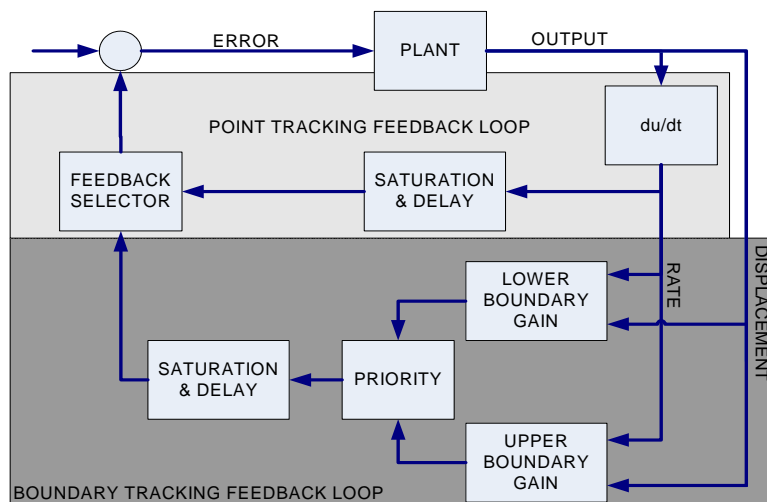


Figure 2. Diagram of Original Boundary Avoidance Tracking Model

2.2.1 Model Assumptions

Five primary assumptions were made that governed the development of Mr. Gray's original model of boundary avoidance tracking. The first was that time-to-boundary was the critical parameter for boundary avoidance tracking (Gray, 2004:12). This parameter was calculated from the system distance and rate to the specified boundary.

$$t_{boundary} = \frac{x_{boundary}}{\dot{x}_{boundary}} \quad (1)$$

Where:

$t_{boundary}$ = time to boundary

$x_{boundary}$ = distance to boundary

$\dot{x}_{boundary}$ = time rate of change of distance to boundary

The use of perceived time first showed promise during a test of nuisance warning criteria in 2001. Using an automated recovery system, pilots were placed in a dive toward the ground. Once the pilot felt that a recovery should occur, he activated the automated recovery system and the aircraft recovered to a safe altitude. Data collected from the test presented a time available to ground impact, or a time to boundary. The times were calculated similarly to the time to boundary presented here (Prosser, 2001:4-5).

The applied boundary tracking gain changed linearly with time-to-boundary and varied between zero and its specified maximum. The larger the time-to-boundary, the

smaller the boundary tracking gain, and vice versa. If the time-to-boundary was greater than the specified time-to-boundary for minimum boundary tracking gain, the boundary tracking gain was zero and the system remained in point tracking. On the other hand, if the time-to-boundary was less than the specified time-to-boundary for maximum boundary tracking gain, it was held at its maximum value.

$$K_{boundary} = \frac{t_{Kmin} - t_{boundary}}{t_{Kmin} - t_{Kmax}} K_{max} \quad (2)$$

Where:

$K_{boundary}$ = instantaneous boundary tracking feedback gain

K_{max} = maximum boundary tracking feedback gain

t_{Kmin} = time to boundary for minimum boundary tracking feedback gain

t_{Kmax} = time to boundary for maximum boundary tracking feedback gain

Note: $t_{Kmin} > t_{Kmax}$

The second assumption was that if the system exceeded a boundary, the maximum boundary feedback gain was held until the system returned within the boundaries (Gray, 2004:12). This assumption allowed for boundary excursions to occur and further assumed that pilots will instinctively maintain the maximum control input possible to return the system below the specified boundary as quickly as possible.

The third assumption was that the pilot was either entirely focused on the point tracking task or the boundary avoidance task – not both (Gray, 2004:12). As shown in Figure 2, the point tracking feedback loop was composed of rate tracking with a simple

gain and time delay. The model simultaneously computed both the boundary tracking feedback and the point tracking feedback and applied only the one with the greatest magnitude.

The fourth assumption was that there was no time delay associated with the switching between point tracking and boundary tracking (Gray, 2004:12). Although some finite amount of time is required for any human to switch from processing one set of information to another, this assumption provided a reasonable first step to modeling boundary avoidance tracking. Furthermore, any additional time delay added to the system would only increase the likelihood of system instability (Gray, 2004:12).

The fifth and final assumption was that both the boundary and point tracking feedback loops have associated gains and maximum feedbacks (Gray, 2004:12) – in other words, each feedback loop is independent of the other. Since pilots inherently limit their control inputs when performing tracking tasks, this assumption allows for more accurately modeling the different types of inputs. When point tracking, pilots limit the magnitude of their inputs to small deflections in an effort to maintain the desired condition for as long as possible. However, when boundaries are present and approached, the magnitude of the deflections can increase greatly; especially if the boundary is approached rapidly and is perceived as hazardous or life-threatening. Under these conditions, pilots can command “stop-to-stop” deflections demanding the maximum performance from the aircraft system. Therefore, by providing a set of gains and associated maximum feedbacks for each feedback loop, the model more accurately reflected the transition between point and boundary tracking.

2.2.2 Point Tracking Pilot Model

A simple pilot model, composed solely of a pure gain and time delay, was implemented to simulate the point tracking portion of the model. As shown in Figure 2, the displacement output was differentiated and sent into the saturation and delay loop of the point tracking feedback loop. Saturation was added to the system in order to limit the applied feedback gain (Gray, 2004:13). The resulting feedback signal from the point tracking pilot model was then fed into the feedback selector.

2.2.3 Boundary Tracking Pilot Model

A similar pilot model, pure gain and time delay, was also used for the boundary tracking feedback loop. However, the gain associated with this loop was a function of the time-to-boundary calculated from the displacement and rate to boundary, as stated in equation 2 and the first and second model assumptions. The resulting feedback signal from the boundary tracking pilot model was then fed into the feedback selector.

The feedback selector compared the magnitudes of the point tracking and boundary tracking feedback loops and fed the larger magnitude into the system plant. This switching mechanism corresponds to the third model assumption where the pilot is either totally involved with the point tracking task or the boundary avoidance tracking, but not both. Overall, both the point tracking and boundary tracking pilot models comprise a single switching-type pilot model that selects the gain necessary for the most pressing tracking task.

2.2.4 System Plant

A simple second order system was used to provide representative aircraft system responses (Gray, 2004:13). The plant was created with a moderate level of damping to simulate the oscillatory response of most aircraft. To excite the plant, a small pulse was input into the system at the onset of the simulation.

2.2.5 Model Results

The values used by the author in both the pilot and plant models were purely notional and were selected to provide examples of the different levels of boundary avoidance tracking. They do not necessarily represent any real system past, present or proposed. They do however represent a system that is driven to an oscillatory behavior as a result of simply shrinking the distances between boundaries. The values selected for the following example are presented in table 1.

Table 1. Boundary Tracking Model Parameter Values

Parameter	Variable	Value
Point Tracking Gain	K_{PT}	0.58
Point Tracking Gain Saturation Limit	$K_{PT-LIMIT}$	0.75
Point Tracking Time Delay	τ_{PT}	0.25 seconds
Maximum Boundary Tracking Gain	K_{max}	0.7
Boundary Tracking Time Delay	τ_b	0.25 seconds
Time-to-boundary for Minimum Boundary Tracking Feedback	t_{Kmin}	0.7 seconds
Time-to-boundary for Maximum Boundary Tracking Feedback	t_{Kmax}	0.3 seconds
Boundary Distance for Example 1 (Point Tracking)	h_{b-1}	0.066
Boundary Distance for Example 2 (Boundary Awareness)	h_{b-2}	0.062
Boundary Distance for Example 3 (Boundary Avoidance)	h_{b-3}	0.0582

The charts shown in Figures 3-5 present the results for three different tracking scenarios. The first plot in each of the figures shows the feedback magnitudes of both the

point tracking and boundary tracking feedback loops. The second plot shows the input signal and the applied feedback magnitude. The third and final plot shows the time history of the tracking event – the relative position of the specified tracking task to the target condition and the position with respect to the applied boundaries. The scales for both feedback magnitudes and relative positions are not included or required for this preliminary analysis as the difference in tracking events are the focus. Finally, all applied boundaries were symmetric in nature; that is they were the same magnitude applied symmetrically about the point tracking target.

The first example was a case of pure point tracking. By setting the boundaries to a relatively large distance (h_{b-1}), the pilot never perceives, or becomes aware of, the imposed boundaries. As shown in Figure 3, the magnitude of the boundary feedback remains zero throughout the event. The system continues to oscillate about the desired point tracking condition and shows the typical exponential decay of a second-order system.

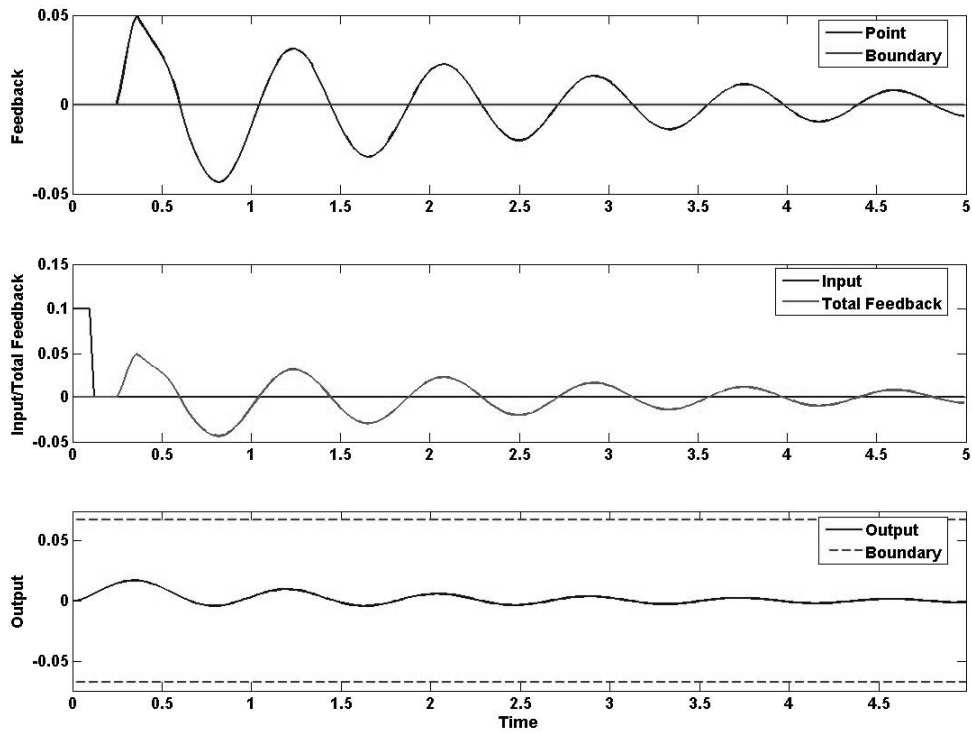


Figure 3. Boundary Tracking Model Result - Point Tracking

The second example, Figure 4, is of boundary awareness. The only model parameter changed here was a relatively small decrease in the boundary distance (h_{b-1} changed to h_{b-2}). Here the relatively closer boundaries cause the pilot to momentarily switch to boundary avoidance tracking to ensure that the boundary has been adequately avoided. Once the boundary has been successfully avoided, the pilot returns to the point tracking task and continues to input to minimize the error associated with the target condition.

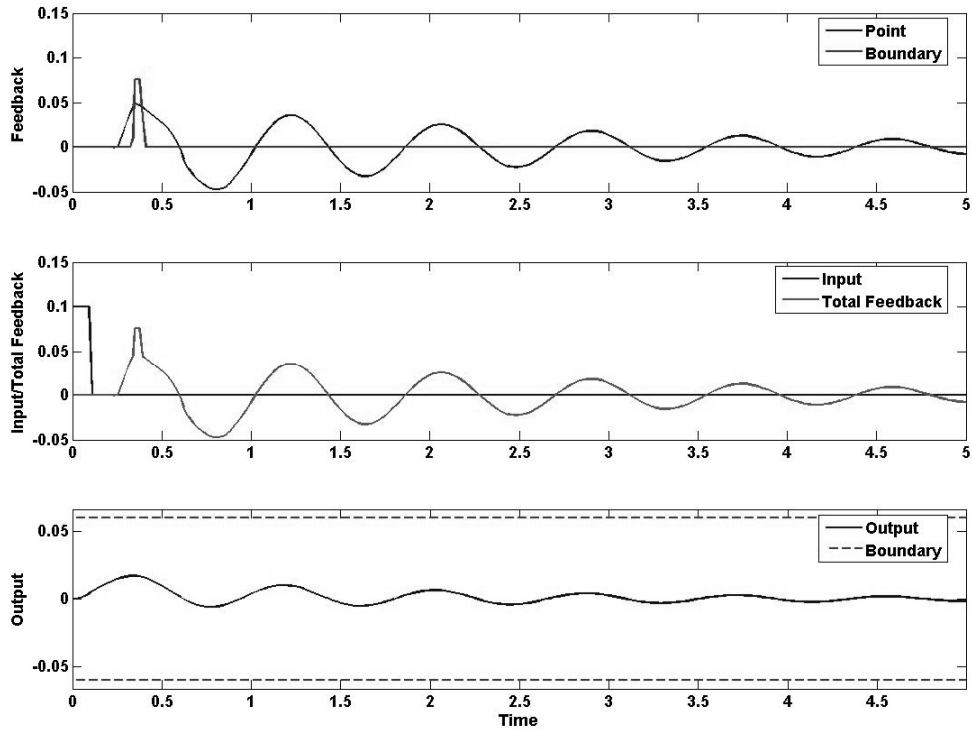


Figure 4. Boundary Tracking Model Result – Boundary Awareness

The transient input associated with the boundary is in fact a boundary avoidance event. What's important with this example is that boundary awareness has occurred. That is, an input was made into the system in an effort to avoid an established boundary. Boundary awareness must occur for boundary avoidance to take place and awareness is governed by the time-to-boundary for minimum boundary tracking feedback gain, t_{Kmin} .

The final example, Figure 5, is of multiple boundary avoidance events. Again the only parameter adjusted for this example was another relatively small decrease in the boundary distance (h_{b-2} changed to h_{b-3}). Here the system oscillations are not solely

caused by the small oscillations of the second-order response, but by repeated inputs resulting from boundary avoidance. The system eventually stabilizes as in the previous two examples and returns to point tracking only. However, larger amplitude oscillations are initially sustained in the system response due to the elevated gains associated with the boundary avoidance events.

From this example, it is apparent that when boundaries are placed sufficiently close to the primary point tracking task, the system can oscillate more frequently and for longer durations than with an unbounded point tracking task. In fact, for the model values presented here, any further decrease in boundary distance results in maximum boundary tracking feedback and system instability with divergent system oscillations.

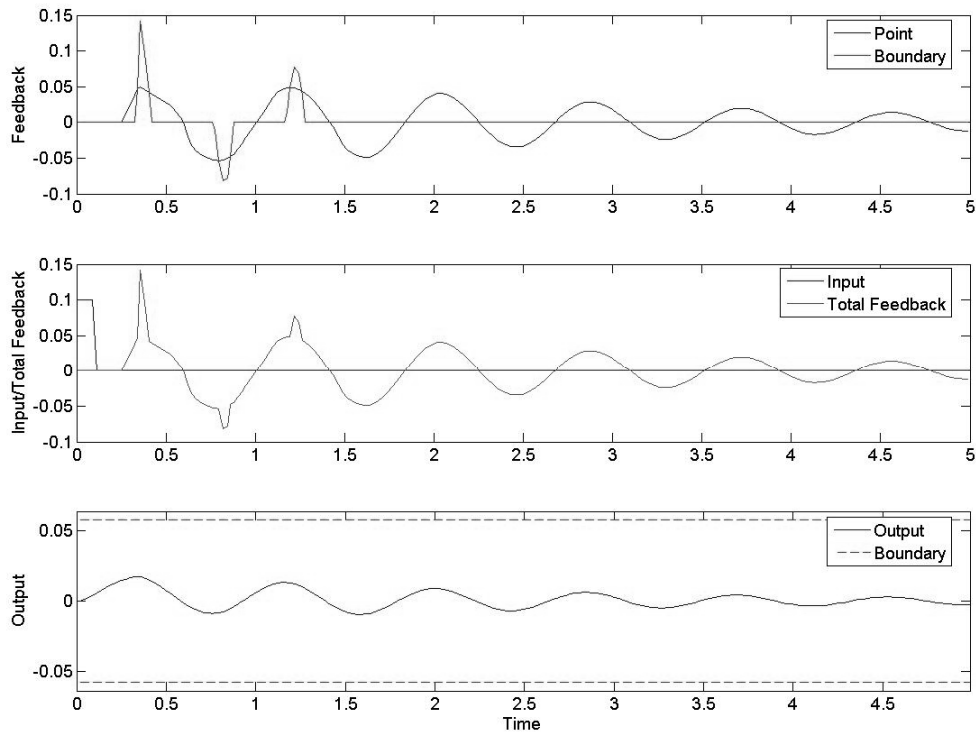


Figure 5. Boundary Tracking Model Result - Boundary Avoidance Tracking

2.2.6 Boundary Avoidance Tracking Modeling Summary

Mr. Gray's initial study proved the ability to successfully model the BAT theory and provided a baseline for identifying the key parameters that characterize boundary avoidance tracking. Holding all parameters constant, it is apparent that increasing the stringency of imposed boundaries can lead to system instabilities and unfavorable aircraft handling qualities. It is essential, therefore, that BAT be more fully investigated and the theory developed to better aid the aerospace community in improving aircraft handling qualities prediction and testing.

The initial model also provided a roadmap for the continued study of boundary tracking. As discussed previously, all the parameters associated with the pilot models and the system plant were variable and not necessarily representative of past, present, or proposed systems. The next steps for investigating boundary avoidance tracking are then to determine representative values of the parameters that characterize boundary avoidance tracking (t_{Kmin} , t_{Kmax} , and K_{max}) and to investigate the relationship between those parameters and the parameters that define the system plant, the flying qualities.

The aircraft flying qualities are indicators of the ability of the closed-loop pilot plus aircraft system to effectively conduct a specified task. If a relationship between these parameters and the parameters that define BAT can be obtained, then a better understanding of the effect that boundary avoidance has on pilot tracking will result. The developed model has already indicated that the mere presence of boundaries affects the stability of a closed-loop system.

2.3 Simulating Boundary Avoidance Tracking

Taking the next step, Mr. Gray developed a pilot-in-the-loop simulation utilizing the flying qualities of a North American Navion (Gray, 2005:6). Developed using Simulink[®], the simulator presented a bounded tracking task to the pilot and recorded the instantaneous stick position for analysis. Eight subjects of varying flight experience each spent approximately 30 minutes in the simulator.

2.3.1 Simulator Tracking Task

The developed task was to match the altitude of a lead Navion that was constantly changing altitude through small amplitude inputs (Gray, 2005:6). The test subjects were

provided with a simple display that provided the relative altitude of the pilot's aircraft with respect to the lead Navion (Figure 6). The goal was to minimize the altitude error between the two aircraft by maintaining the aircraft altitude line on the zero reference and simultaneously avoiding the boundaries.

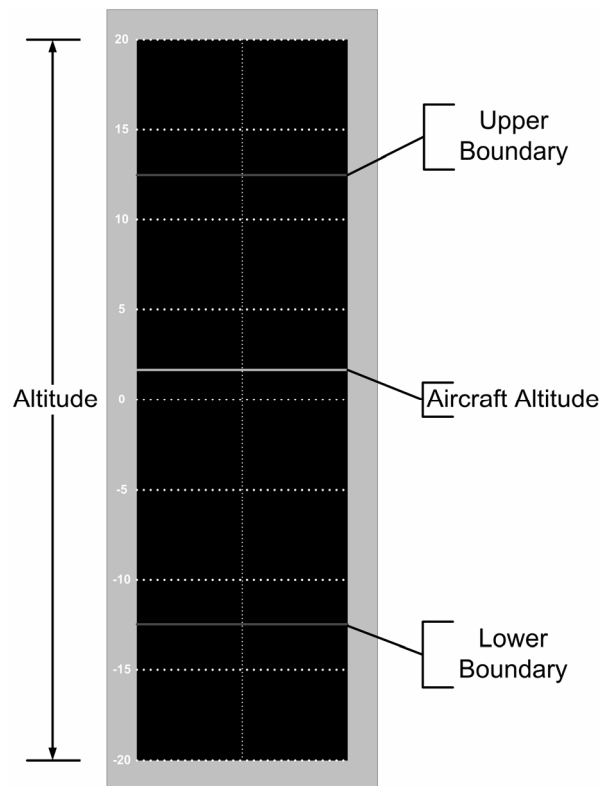


Figure 6. Gray Simulator Tracking Task Display

The boundaries were brought 25% closer to the zero reference every minute and the oscillatory flight path of the lead Navion was also repeated every minute. Each subject flew three different scenarios: first, the standard Navion tracking task; second, a 300 millisecond time delay added to the pilot's inputs; and third, a 0.3 radian per second

rate limit placed on the deflection of the horizontal tail (Gray, 2005:6). The simulation was stopped once a boundary was crossed.

2.3.2 Simulator Data Reduction

All data from the pilot-in-the-loop simulation was collected at a rate of 100 samples per second. The key boundary tracking parameters (t_{Kmin} , t_{Kmax} , K_{max}) were determined by applying the previously developed boundary tracking model to the collected simulator results. The key parameters, along with the pilot time delay, were varied until the model results closely matched the simulator data.

2.3.3 Simulator Results

A total of 27 boundary avoidance events were evaluated. For events that lasted 60 seconds or longer, the values of t_{Kmin} and t_{Kmax} were both found to possess a strong central tendency. For t_{Kmin} , the mean was 2.8 seconds with a variance of 0.25 seconds. The mean for t_{Kmax} was 0.3 seconds with a variance of 0.04 seconds (Gray, 2005:11).

The maximum boundary tracking feedback gain was found to correlate well with the test subject's ability to track for a long duration. The most interesting results were provided from a developed parameter, termed the boundary tracking parameter (BTP).

$$BTP = \frac{t_{Kmin} - t_{Kmax}}{K_{max}} \quad (3)$$

This parameter showed some potential correlation with the length of successful tracking time. As the BTP value increased, so did the duration of the successful tracking time (Figure 7). This result makes intuitive sense in that as pilots are able to limit the magnitude of their inputs, and their associated gains, they are able to maintain system

stability longer and successfully perform the tracking task for a longer duration. Also, while holding the pilot gain constant, as the difference between t_{Kmin} and t_{Kmax} decreases, so too does the duration of the successful tracking time. This makes sense in that if the difference between these two parameters is too small, the pilot will then rapidly transition to a maximum input and cause the system to become unstable more rapidly (Gray, 2005:11).

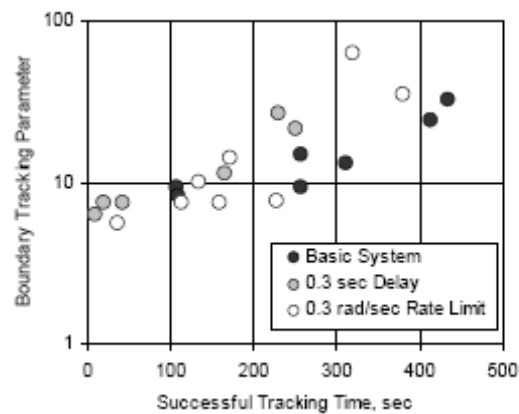


Figure 7. Boundary Tracking Parameter (BTP) Results (Gray, 2005:11)

Overall, the results of Mr. Gray’s simulator study provided for an initial characterization of BAT. Perception of time-to-boundary appears to be an inherent human characteristic and the more experienced and less aggressive the pilot, the more successful the ability to track in the presence of boundaries. These results lay the foundation for the research that was conducted for this thesis.

3. Research Objectives and Experiment Methodology

3.1 Research Overview

3.1.1 System Definition

In order to properly evaluate the effect of BAT, it is important to begin by defining the system that was investigated. The system under experimentation for this research was the complex pilot plus aircraft system. Termed “the pilot’s-eye system”, this system comprised all the steps between the pilot’s perception of an impending boundary and the aircraft response from the pilot’s system inputs. Significant parts of the system included the pilot’s eye, brain, and hands, the aircraft control stick’s tactile feedback mechanisms, the flight control system, and the aircraft aerodynamics. Use of this system was critical to characterizing the time-to-boundary parameters as they are functions of pilot perception and response.

In order to faithfully represent the pilot’s system feedback, a video camera system was used to capture the pilot’s perspective of the tracking task as closely as possible. Data recorders were also used to capture the pilot’s system inputs.

The T-38C aircraft, originally produced by Northrop Corporation, Aircraft Division and upgraded by The Boeing Company, is a two-place, twin-turbojet supersonic trainer. The aircraft is equipped with an all-movable horizontal tail and a hydraulically powered, irreversible flight control system. The control surfaces are non-reversible, so conventional aerodynamic feel in the control stick was provided artificially by springs and bobweights.

3.1.2 Boundary Avoidance Tracking Parameters

As stated in Chapter 2, time-to-boundary was assumed to be the critical parameter in characterizing BAT. The key times-to-boundary are t_{Kmin} , for the time-to-boundary at minimum boundary tracking gain and t_{Kmax} , for the time-to-boundary at the maximum BAT gain. Physically, the parameter t_{Kmin} corresponds to the perceived time-to-boundary at which a pilot first responds to the boundary by making an input into the system. The t_{Kmax} parameter then refers to the time-to-boundary at which the pilot applies a maximum system input to avoid the impending boundary.

The BAT gain, which is the magnitude of the system input by the pilot, is a result of the pilot's perceived time-to-boundary. As shown in equation 2, the BAT gain was assumed to vary linearly between t_{Kmin} and t_{Kmax} from zero to a maximum value. Therefore, it is the maximum BAT gain, K_{max} , that is of interest in helping to characterize BAT events.

The boundary tracking parameter (BTP), which combines all three parameters into a single parameter, was also of interest. It was thought that this parameter acted as a normalizing agent. The results of the research did not confirm this assumption. More experienced pilots will typically allow themselves to react to a boundary at a smaller time-to-boundary than less experienced pilots. Likewise, more experienced pilots will limit their system inputs to smaller magnitudes while neophytes will typically use much larger inputs.

Finally, of interest was the frequency at which the pilot moved the longitudinal stick during BAT events. This pilot actuation frequency, ω_{BAT} , would be used for

frequency domain analysis of the system to determine how closely the pilots were operating to the system crossover frequency – the frequency at which the system has a phase of -180° . Applying the definition – “A PIO exists when the airplane attitude, angular rate, or normal acceleration is 180 degrees out of phase with the pilot’s control inputs” (Mitchell and Hoh, 1995:18) – the airplane attitude can be considered analogous to the pilot’s perceived relative position. As such, comparison of ω_{BAT} with the system crossover frequency will provide a result of system PIO sensitivity. Once all of the BAT parameters had been determined and characterized, correlating them with the aircraft flying qualities could be carried out.

3.1.3 Aircraft Flying Qualities

Flying qualities are the parameters that characterize the dynamic behavior of a piloted aircraft. Through several decades of research and flight test, countless parameters have been developed to better understand, predict, and model aircraft flying qualities in an effort to provide aircraft that exhibit desirable characteristics. Though initial research into boundary avoidance tracking provide for a single time-to-boundary for boundary awareness and a single value of time-to-boundary for maximum boundary feedback gain across a wide range of pilot experiences, the effect that the aircraft’s flying qualities have on the boundary tracking parameters has never been investigated. Finding a correlation or an independence between these parameters will ultimately lead to better characterization and understanding of BAT and the effect it has on pilot tracking success.

As a first step into the investigation of the relationship between the BAT parameters and flying qualities, two parameters were selected based on Mr. Gray’s

previous work and based on classical systems analysis. The first parameter was the system time delay, τ_{delay} – the difference in time from the system input to associated system motion. Excessive system time delay is known to be a contributor to poor aircraft handling qualities and was identified in Mr. Gray’s simulator study as a contributing factor to decreased successful tracking times (Gray, 2005:11).

The second parameter was the system crossover frequency, ω_{180} – the frequency at which system input is 180 degrees out of phase with system output. This parameter was of interest in comparison with the pilot actuation frequency, ω_{BAT} . If the pilots were operating at or near the crossover frequency during BAT events, the system could be unstable and lead to undesirable aircraft oscillations.

All of the research parameters of interest have been defined for the pilot’s-eye system of interest. The parameters, t_{Kmin} , T_{Kmax} , K_{max} , BTP , and ω_{BAT} will be determined and analyzed in order to characterize BAT. Then the aircraft flying qualities parameters, τ_{delay} and ω_{180} , will be determined and correlated with the BAT parameters to see what the effect is on pilot tracking success.

3.2 Experiment Design

The techniques developed to collect the parameters of interest were centered around the specified point tracking task. In this section, the details of that tracking task, the mindset of the pilots during the tracking task, and the conditions for the experiment will be discussed.

3.2.1 Pilot Tracking Task

The point tracking task was simple: fly a specific formation position off the target aircraft by tracking reference markings and maintain the target aircraft's wingtip within the specified boundaries. The reference markings for the point tracking task were to maintain the front corner of the wingtip of the target aircraft level with the star in the chevron on the fuselage (see Figure 8). The reference markings for the boundaries were the solid and dashed lines immediately above and below the chevron. The basic formation position for the experiment approximated a "route" position with approximately ten foot wingtip spacing. The pilot continued the point tracking task throughout the test point, abandoning it only when boundary penetration was perceived to become a threat, or the test point was terminated (if the tracking task could be continued without any boundary avoidance tracking or due to exceeding the databand).

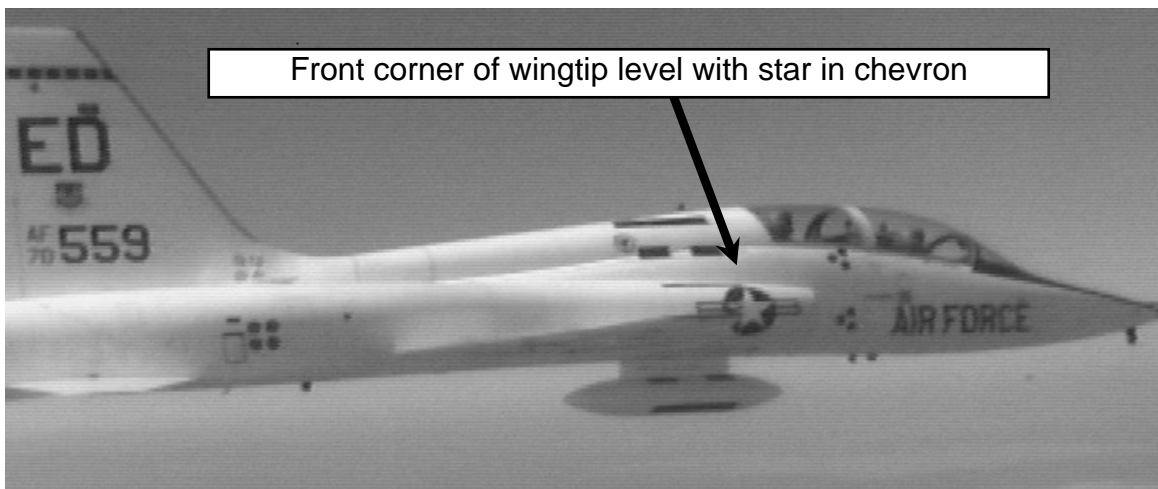


Figure 8. Tracking Task Visual Reference

3.2.2 Pilot Mindset

Because of the inescapable human element of the experiment, the individual pilots could possibly generate different results while performing the tracking tasks under similar conditions. Control aggressiveness, reaction speed, and self-limitation (self-imposed limits to avoid over-g or excessive buffet) could potentially vary widely from pilot to pilot. Because the pilot was a key factor in the experiment, tracking task data were obtained from all of the pilots at each test condition.

In an attempt to faithfully recreate the stress of a pilot who perceives an oncoming hazard, the test pilots flew with a specific mindset: allowing the wingtip to deviate beyond the imposed horizontal boundary markings was unacceptable. With real aircraft structural and operational limits in mind, the pilots would naturally limit the magnitude of their inputs. To alleviate this potential additional boundary, the experiments were designed to remove or reduce the risk of exceeding load factor limits. This allowed the pilots to maneuver with minimal restraint.

3.2.3 Flight Conditions

Without a variable stability aircraft, the flight conditions of the experiment had to be varied in order to provide a range of aircraft flying qualities for analysis. The aerodynamic effects of the system were altered by performing the flight test techniques at different altitudes, airspeeds, and landing gear configurations to cause differences in the aircraft flying qualities. The flaps and speed brakes were not extended for any test points. Table 2 lists the test conditions used for this experiment.

Table 2. Summary of Flight Conditions

Flight Condition	Altitude (feet)	Landing Gear Position	Airspeed (KIAS)	Typical Mach
High Fast Cruise	20,000	Up	375	0.80
High Slow Cruise	20,000	Up	250	0.55
High Configured	20,000	Down	210	0.46
Low Fast Cruise	10,000	Up	375	0.67
Low Slow Cruise	10,000	Up	250	0.45
Low Configured	10,000	Down	210	0.38

3.3 Fixed-Base Simulation

In order to properly prepare for the experiment, a simulator was used by the flight test team to develop flight test techniques for both aircraft flying qualities and boundary avoidance tracking. The simulator was developed by Lieutenant Jay Kemper of the Air Force Research Laboratory Air Vehicles Directorate (AFRL/VA) over a one year period.

3.3.1 Simulator Properties

The T-38A simulator was provided by the Air Force Aeronautical Systems Center (ASC) Training Aircraft Group T-38 Systems Squadron. The simulator was a full non-linear six degree of freedom simulation of a T-38A aircraft programmed in the ADA programming language.

Unfortunately the AFRL/VA simulators were not able to utilize the ADA simulation. Lieutenant Kemper developed both a modified version of the ADA-based

simulation as well as a communications algorithm that allowed the AFRL/VA simulators to successfully execute the T-38A simulation. This effort was crucial to the success of both a highly functional and high fidelity T-38A simulator and the development of experiment specific flight test techniques.

The Infinity Cube simulator provided a full 180 degrees of visibility with full look-up capability through the use of four independent video projectors. The aircraft inceptors were, however, not indicative of the controls found in a T-38 aircraft. The simulator was configured for simulation of F-16 aircraft with a force-feedback side stick and a single throttle control. As T-38 aircraft use a movable center stick and two throttle controllers, the cockpit inceptors were not representative of what the flight test team would be using during the experiment. Furthermore, the graphical display of the simulator could not be altered to provide representative visual boundaries that would be used during the experiment.

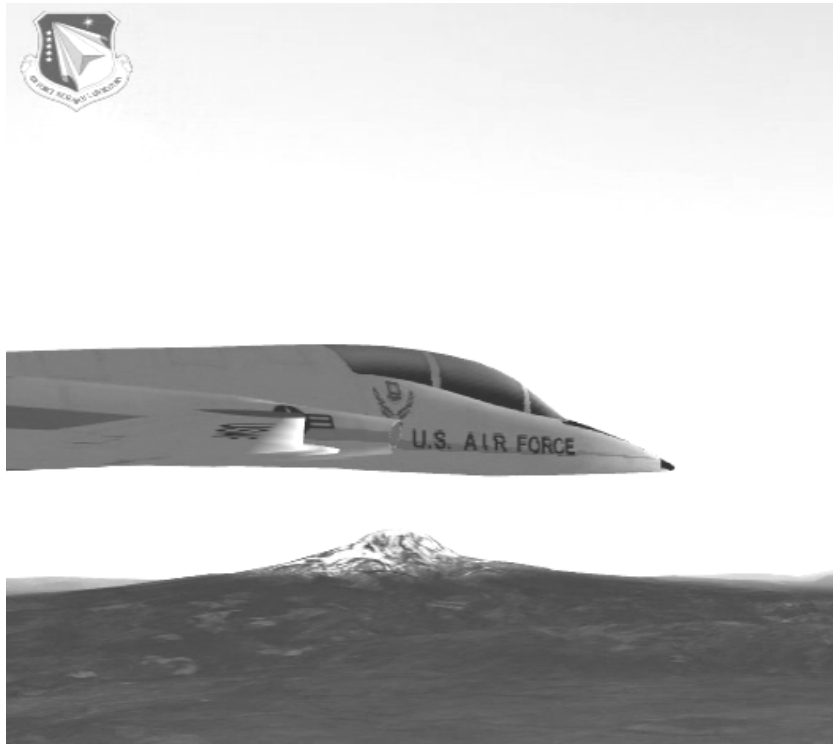


Figure 9. AFRL Simulator Visual Presentation (Left Panel Display)

Overall, though, the test pilot flight crew members reported that the aircraft response and handling qualities were good representations of actual T-38A aircraft. The visual presentations (Figure 9) provided the flight crew members with an excellent representation of the flight conditions that would be experienced during the execution of the experiment. For the use of flight test technique development, the AFRL/VA developed T-38A simulator was an excellent resource that saved valuable experiment flight time.

3.3.2 Aircraft Flying Qualities Flight Test Technique Development

Utilizing the pilot's-eye system, flying qualities flight test techniques had to be developed that were indicative of the pilot plus aircraft open-loop system. For the system time delay parameter, the technique selected was a traditional time delay technique – application of a step input followed by measurement of the delay from the time of the input to the first aircraft response. Trial of this technique in the simulator showed the maneuver was quick and easy to replicate. A few iterations of this technique by each test pilot provided confidence in the execution of the maneuver and gave the test team a better feel for the time required for test point set-up, execution and the maneuvers required for reestablishing the formation.

To capture the system crossover frequency, the traditional frequency sweep flight test technique was modified to reflect the difference in traditional aircraft systems and the pilot's-eye system. In traditional frequency sweeps, the pilot slowly moves the aircraft stick forward and aft to induce aircraft motion. The pilot then begins to increase the frequency of the forward and aft inputs so that a wide range of frequencies are covered and frequency domain analysis tools can be applied.

For the pilot's-eye system used in the experiment, the frequency sweep inputs were similar to those as described in the traditional frequency sweep. However, the system output was defined as the relative altitude difference between the target aircraft and the test aircraft. So, pilot inputs were applied with the traditional technique and the system output measured from the visual data captured by the camera system.

3.3.3 Boundary Avoidance Tracking Flight Test Technique Development

As described in the pilot task section, the goal of the pilot was to maintain the target aircraft wingtip in the center of the chevron and prevent the wingtip from crossing any imposed boundary. The development of a mechanism to provide an approach to boundaries was also necessary to excite potential BAT events. As such, two methods were chosen – decreasing boundary distances and target aircraft maneuvering.

The decreasing boundary method required that the target aircraft remain at the specified flight condition and configuration while the test aircraft gradually decreased the boundary distances. To simulate this, the test pilots utilized the top and bottom of the target aircraft's fuselage just above and below the chevron (see Figure 9) as well as the top and bottom of the blue circle in the chevron. All pilots found it relatively easy to maintain the desired formation position even as the boundary distances were decreased during the simulations. Though this method rarely produced a BAT event or aircraft oscillation in the simulation, it was adopted for use in the experiment as a baseline maneuver. This maneuver was termed the stable platform maneuver.

The target aircraft maneuvering methods provided the best results in the simulator for BAT events. The overall premise for these types of maneuvers was to have the target aircraft perform a maneuver that would create a perceived approach to a boundary by the test pilot. Three separate maneuvers were developed in the simulator. The first maneuver, termed the pull-up, was a simple method for creating an approach to the boundary located below the target chevron. The pull-up required the target aircraft to pull to 1.5 Gs within 2 seconds and maintain the pitch attitude. This maneuver caused the

target aircraft to begin a climb which the pilot of the test aircraft perceived as an approach to the lower boundary.

The second maneuver, termed the push-over, was similar to the pull-up, except the target aircraft performed a push to 0.5 G within 2 seconds and maintained the pitch attitude. The push-over created an approach to the boundary located above the target chevron. Both the pull-up and push-over maneuvers showed great success in the simulator and were very easy to set-up and execute. The test pilots again utilized the top and bottom of the fuselage and the top and bottom of the blue circle in the chevron as boundaries during the simulation producing repeated BAT events.

The third maneuver, termed the rollercoaster, was a combination of both the pull-up and the push-over and was derived from the simulator study conducted by Mr. Gray (Gray, 2005:6). The rollercoaster had the target aircraft begin from steady level flight and then perform a series of pull-ups and pushovers. The series began from 1 G with a ± 0.1 G pull-up/push-over and then increasing by ± 0.1 G to a maximum pull-up of 1.5 G and a minimum push-over to 0.5 G. No G rate was specified for the maneuver. Once that level was reached, the series then reversed and gradually returned to 1 G. This maneuver always produced BAT events and divergent oscillations by all pilots for all boundaries in the simulator. This was by far the most dynamic of the target aircraft maneuvering methods evaluated in the Infinity Cube simulation. Table 3 below summarizes all of the flight test techniques developed for the experiment.

Table 3. Summary of Developed Flight Test Techniques

Maneuver	Area	Description
System Time Delay	Flying Qualities	Step input until aircraft motion was evident; measured time lag from input to aircraft response
Frequency Sweep	Flying Qualities	Increasing frequency of longitudinal inputs; system response measured visually as change in relative altitude
Stable Platform	BAT	Target aircraft remained stable and non-maneuvering; test aircraft gradually decreased boundaries until smallest boundaries reached or boundary excursion occurred
Pull-Up	BAT	Target aircraft performed pull-up to 1.5 G within 2 seconds; test aircraft perceived approach to lower boundary and responded
Push-Over	BAT	Target aircraft performed push-over to 0.5 G within 2 seconds; test aircraft perceived approach to upper boundary and responded
Rollercoaster	BAT	Target aircraft performed varying pull-up and push-over maneuvers; test aircraft perceived repeated approaches to both upper and lower boundaries

3.4 Experiment Instrumentation

The target aircraft used for the experiment were marked with two types of decals for both pilot tracking and for post-flight data analysis. The test aircraft was equipped with both a camera system for recording a pilot's-eye representative visual image of each event as well as an integrated data acquisition system to capture aircraft stick displacement. Each item is detailed in the following sections.

3.4.1 Aircraft Visual Markings

Two types of visual markings were required on the target aircraft for the experiment. The first were boundary lines that would be referenced by the pilot of the test aircraft for each of the maneuvers. The second type was target markings designed to aid an automated visual tracking algorithm. These markings are shown in Figure 10 which depicts the target aircraft during an experiment flight.

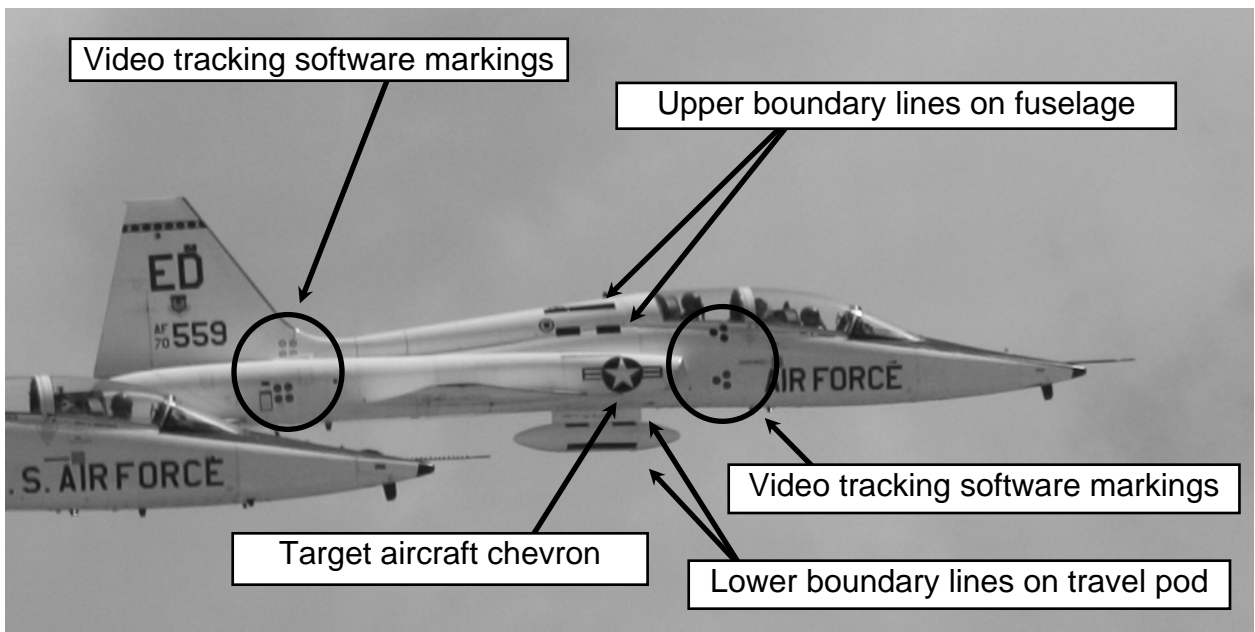


Figure 10. Target Aircraft Visual Markings

The first type of markings, the boundary lines, are shown in Figure 10 as solid and dashed black lines located on the fuselage and travel pod of the target aircraft. These lines were the boundaries that the pilot of the test aircraft used during each of the maneuvers. A third set of boundaries was also established if smaller boundary distances

were required. These boundaries were the top and bottom of the circle in the chevron on the target aircraft, the same boundaries previously established in the fixed-based simulator.

The second type of markings, the video tracking software markings, were specially designed for use with an automated video tracking algorithm. These red and yellow series of dots would be automatically located in each video frame allowing for boundary position information to be provided for further data analysis. Since the wingtip position was also required for analysis, a green decal was used to allow the video tracking algorithm to autonomously track its position. As can be seen in Figure 10, the wingtip on the T-38A was extremely thin and difficult to see even with a bright green decal. This led to severe problems with post-flight data reduction which is discussed in detail in Chapter 4.

3.4.2 Aircraft Mounted Camera System

To capture the visual stimuli of the pilot's-eye system as closely as possible, a camera system was installed immediately behind the ejection seat of the front cockpit. This aircraft mounted camera system was approximately three feet behind and slightly higher than the eyes of the pilot, as shown in Figure 11.

The camera was fixed into position by a bracket so some amount of trial and error was required to properly align the camera's field of view; however, once calibrated the camera required no maintenance or recalibration throughout the testing. The installation of the aircraft-mounted camera was a minor modification that integrated the camera with the aircraft electrical system for power and with three 8mm tape decks in the rear cockpit.

One tape recorded the production aircraft HUD/MFD feed, the second recorded the aircraft-mounted camera feed, and the third recorded the data acquisition system data. All three tapes contained a time stamp for data synchronization. The video frame rate was 30 frames per second.

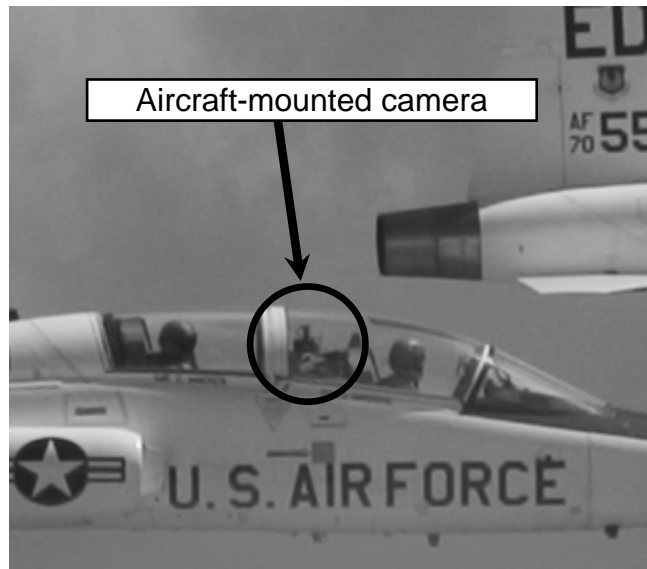


Figure 11. Aircraft Mounted Camera Placement

A helmet-mounted camera system was used on every flight during the experiment in an effort to more closely capture what the pilot was viewing during each event. The system was comprised of a small lipstick-style camera attached to the pilot's helmet, a video tape recorder, and batteries which were self-contained in a modified survival vest and worn by the pilot during each flight. Unfortunately, the system rarely captured the target aircraft fully in the field of view despite repeated calibrations and adjustments. Though not directly at the pilot's point-of-view, the video obtained from the aircraft-

mounted camera system was a very close representation of what the pilots viewed and was an excellent substitute for a helmet-mounted system.

3.4.3 Aircraft Data Acquisition System

The aircraft data acquisition system (DAS) recorded multiple aircraft parameters during each flight. However, only four parameters were needed for this experiment – longitudinal stick position, aircraft load factor at the pilot’s location, indicated airspeed, and aircraft pitch attitude. All data parameters were recorded at a rate of 20 samples per second with the longitudinal stick position data provided in units of degrees, load factor in Gs, indicated airspeed in knots, and pitch in degrees.

4. Analysis and Results

4.1 Research Assumptions

Before going into the analyses and results of the collected data, it is important to introduce two primary assumptions that governed both the reduction of the data and the analyses resulting from the data reduction.

4.1.1 Aircraft Mounted Camera

The aircraft mounted camera system was assumed to be representative of the pilot's viewpoint. Comparison of the collected video footage from a helmet mounted camera and the aircraft mounted camera showed that the differences between the two viewpoints were minor. This was also confirmed by the test pilots after their review of the aircraft mounted camera footage.

This assumption allowed for the use of the visual data collected by the aircraft mounted camera system to represent the error signal in the pilot's-eye system. The aircraft mounted camera footage was more reliable than the helmet mounted camera and also provided a much more stable image. Even though the aircraft mounted camera was placed approximately three feet behind the pilot's head, this system provided accurate and reliable visual data for analysis of BAT events in the pilot's-eye system.

4.1.2 Vertical Motion Constraint

The second primary assumption was that the relative motion of the target and test aircraft was constrained to the vertical axis. This assumption was made as a result of the tracking task, applied boundaries, and developed flight test techniques all being constrained to the aircraft longitudinal axis. As such, the assumption was that the motion

captured on the aircraft mounted camera would be primarily vertical in nature. This was later confirmed after reviewing the collected video footage.

The driver for this assumption was the reduction in the complexity of the data reduction algorithm for the collected video data. By limiting the reduction to a single axis, the development of the algorithm to determine the distance to boundary was greatly simplified. Again, after reviewing the collected video footage, this assumption was accurate and had little impact on the quality of the reduced data.

4.2 Data Reduction Algorithms

Data reduction tools consisted of both commercial off-the-shelf software and locally created MATLAB[®] routines. Each served a specific purpose in reducing the separate streams of data and integrating them into the required data products for analysis. After each flight, data reduction generally followed two tracks in parallel: one for the video data, and one for the stick deflection data. The two data streams were integrated at the last step to produce the final data products for analysis. Figure 12 illustrates the flow of data through the data reduction process.

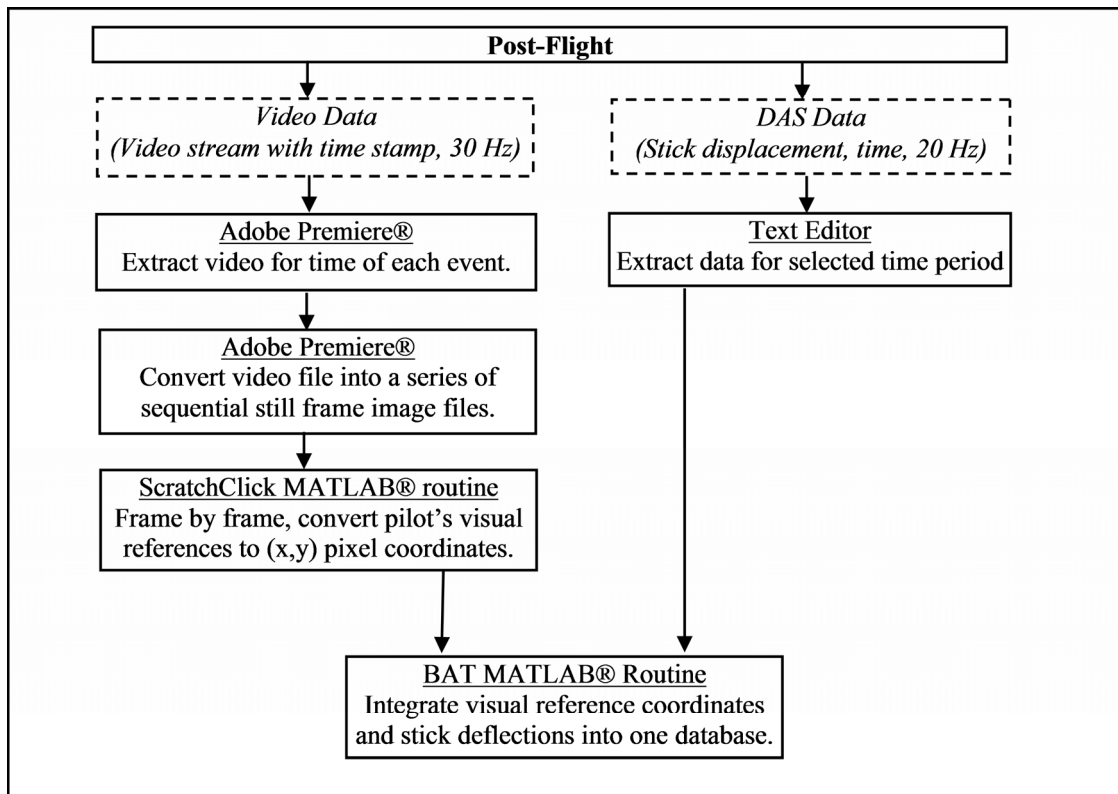


Figure 12. Data Reduction Flow Chart

The onboard camera used to capture the pilot's perspective stored the captured images on an analog tape. To process the video digitally, a commercial off-the-shelf video tape player converted the analog signal to an uncompressed version of the Audio Video Interleave (AVI) file format and digitally exported the file to a computer via an Institute of Electrical and Electronics Engineers (IEEE) standard 1394 bus also known as FireWire.

Once the analog file was converted to a digital format, Adobe Premiere® was used to reduce the typical 14 gigabyte video file into a more manageable 2 gigabyte size.

This was done by deleting the nonessential portions of the typical 1 hour and 15 minute flight. These portions included all events except the actual test points which were typically 10 to 15 seconds long. The end result was a reduction of the flights video length from 1 hour and 15 minutes to roughly 7 minutes. Two seconds of video data prior to the beginning of the maneuver were collected as a buffer to determine trim information and the clip was ended at either the termination of the maneuver or when the aircraft departed the field-of-view (FOV) of the camera. The 15 to 17 minute AVI clip contained all the pertinent events of the sortie but was still in video format. To analyze each individual 10 to 15 second event, the AVI clip was parsed and converted into a 30 frames-per-second (fps) still image sequence and saved in individual folders descriptively labeled to organize and separate individual events.

4.2.1 Automated Visual Tracking Routine

Collected video data were processed immediately following each flight. Once converted to AVI format, the video events were first processed, using Adobe Premiere, through three chromatic filters to help eliminate background clutter and other noise items. A red filter was used to isolate the upper marks, a yellow for the lower marks and a green filter was used to isolate the wingtip. Figure 13 illustrates a pre-processed frame (on the left) and that same frame after the chromatic filtering process (shown on the right). The chromatic filter image output is a black-and-white AVI which optimizes the video for processing in Matlab[®]. Each of these three files were processed through a Matlab[®] routine that determined time histories of wingtip position, boundary positions, and wingtip rates relative to these boundaries positions.

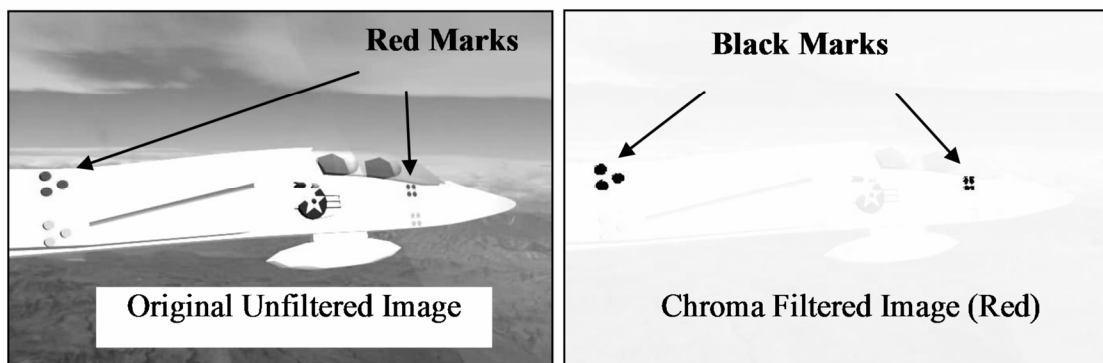


Figure 13. Chromatic Filtering of Visual Data

The developed Matlab[®] visual tracking algorithm applied a vanishing point technique to determine the location of the boundaries in each frame of video data. The red and yellow markings defined two horizontal parallel lines that on a two-dimensional frame of video appear to intersect at some distant point, the vanishing point. Once the location of the vanishing point was determined, the location of the boundaries could be determined from a line drawn from the vanishing point to the boundaries on the aircraft.

With the boundaries defined, the location of the wingtip was determined by tracking the pixel position of the green chroma filtered image. Unfortunately, this is where the automated tracking algorithm broke down. The wingtip of the T-38 aircraft is very narrow. Even with a distinctive green marking, the aircraft mounted camera system did not possess adequate resolution to identify the wingtip in each frame of the collected video data. This prevented the automated tracking algorithm from tracking the wingtip position.

The next step was to apply the automated algorithm to at least determine the location of the boundaries and then manually determine the location of the wingtip. However, the location of the vanishing point was extremely noisy and at an extreme distance. This prevented an accurate determination of the location of the boundaries on the target aircraft. Coupling this with the inability to accurately determine the wingtip position automatically, a manual data reduction algorithm was required to extract the information from the visual data.

4.2.2 Manual Visual Data Reduction Routine

A manual visual data reduction tool was developed by Maj. Scott Heritsch, a member of the flight test team, to aid in the extraction of data from the collected video images. The tool, named ScratchClick, was a Matlab[®] GUI routine that allowed the user to select specific points on each frame of video and save the pixel locations for further analysis. To determine the time-to-boundary as perceived by the pilot, six points of interest per frame were required: one at the leading corner of the target aircraft wingtip, one at the tracking reference where the wingtip was to be maintained, and two to define each linear boundary above and below the tracking reference. Figure 14 illustrates the ScratchClick interface as well as how ScratchClick displayed these six points. From this information the vertical distances from the tracking point to the wingtip and to each boundary were calculated.

A significant amount of visual data was collected during the course of the flight test. As such, only approximately 30% of the total data was reduced and analyzed during this research.



Figure 14. Example ScratchClick Interface for Visual Data Extraction

4.2.3 Aircraft Data Acquisition System Routine

The data collected by the aircraft data acquisition system (DAS) was collected via an 8mm tape. The data was then converted from binary to numerical data for analysis. Once each event was determined in the reduction of the video data, the DAS data was parsed to match the duration of the video data.

4.3 Aircraft Flying Qualities Parameter Analysis

4.3.1 Determination of System Time Delay

To obtain the system time delay data, the test aircraft stabilized in the point tracking formation position off of the target aircraft. The target aircraft provided a stable reference platform by maintaining straight and level, unaccelerated flight. When cleared to maneuver, the pilot of the test aircraft performed an aft stick step input.

The system time delay was calculated as the length of time between two events: the pilot's initial movement of the stick from the trim position, and the initial response of the aircraft. Definite stick movement was determined by a rapid stick deflection beyond the noise levels observed while stabilized in the trim condition. The step inputs were of sufficient quality to readily identify the moment the input was commenced. The system time delay was determined by overlaying the time history of the longitudinal stick position on the collected video. The time at which the step input was made was recorded and then the time at which visible aircraft motion first began was recorded. The difference in these two values was recorded as the system time delay. Table 4 summarizes the system time delays for each flight condition. The time delay values were calculated from one test run at each condition.

Table 4. System Time Delays

Flight Condition	Altitude (feet)	Landing Gear Position	Airspeed (KIAS)	System Time Delay (seconds)
High Fast Cruise	20,000	Up	375	0.07
High Slow Cruise	20,000	Up	250	0.17
High Configured	20,000	Down	210	0.30
Low Fast Cruise	10,000	Up	375	0.03*
Low Slow Cruise	10,000	Up	250	0.10
Low Configured	10,000	Down	210	0.17

* Note: The data sampling rates limited the precision of the system delays when less than 1/20 of a second.

4.3.2 Determination of System Crossover Frequency

The system crossover frequency, ω_{180} , is defined for this experiment as the rate at which an oscillatory pitch input by the pilot results in the opposite vertical movement from the aircraft. When cycling the stick at this frequency, the aircraft will climb during forward stick application and descend during aft stick application because the aircraft is still responding to the previous input. If the pilot's input is slower than the crossover frequency, the aircraft will follow the stick inputs (aft stick results in a climb, as one would expect); if the pilot's input is faster, the aircraft does not have enough time to respond to the rapidly alternating commands and remains nearly level at the trim state. The system crossover frequency is of interest because if the pilot makes repeated corrections at this rate (such as when bouncing between two opposing boundaries), the aircraft may move in a direction opposite what the pilot is commanding and anticipating. Such a situation increases the potential for divergent oscillations and PIOs.

To determine the system crossover frequency, the test aircraft performed a frequency sweep in pitch while at or near the standard formation position off the target aircraft. To perform the frequency sweep, the pilot made slow, alternating inputs of small stick deflections and gradually increased the frequency. Once the pilot perceived the aircraft vertical movement to be out of phase with the stick deflection, the pilot dwelled at that frequency to record a sufficient stick trace on the DAS for later analysis. Throughout the frequency sweep, the pilot adjusted stick deflections to keep the target aircraft within the field of view of the aircraft-mounted camera for post-flight video analysis. Post-flight analysis entailed measuring the period of the longitudinal stick oscillations and taking the reciprocal to determine ω_{180} . The measured system crossover frequencies are listed in table 5.

Table 5. System Crossover Frequencies

Flight Condition	Altitude (feet)	Landing Gear Position	Airspeed (KIAS)	System Crossover Frequency (Hz)
High Fast Cruise	20,000	Up	375	0.88
High Slow Cruise	20,000	Up	250	0.59
High Configured	20,000	Down	210	0.56
Low Fast Cruise	10,000	Up	375	0.71
Low Slow Cruise	10,000	Up	250	0.45
Low Configured	10,000	Down	210	0.45

4.4 Boundary Avoidance Tracking Characterization

4.4.1 BAT Data Analysis Tool

The reduced data from both the aircraft mounted camera system and the aircraft data acquisition system had to be collated to fully analyze each BAT event. A Matlab[®] graphical user interface (GUI) tool, BAT_Calc, was created to pull both the visual data and the DAS data together and provide a single interface to determine all of the parameters of interest. Figure 15 shows the BAT_Calc tool that was developed. There are several displays and controls on this tool, and each will be discussed more fully in the sections that follow.

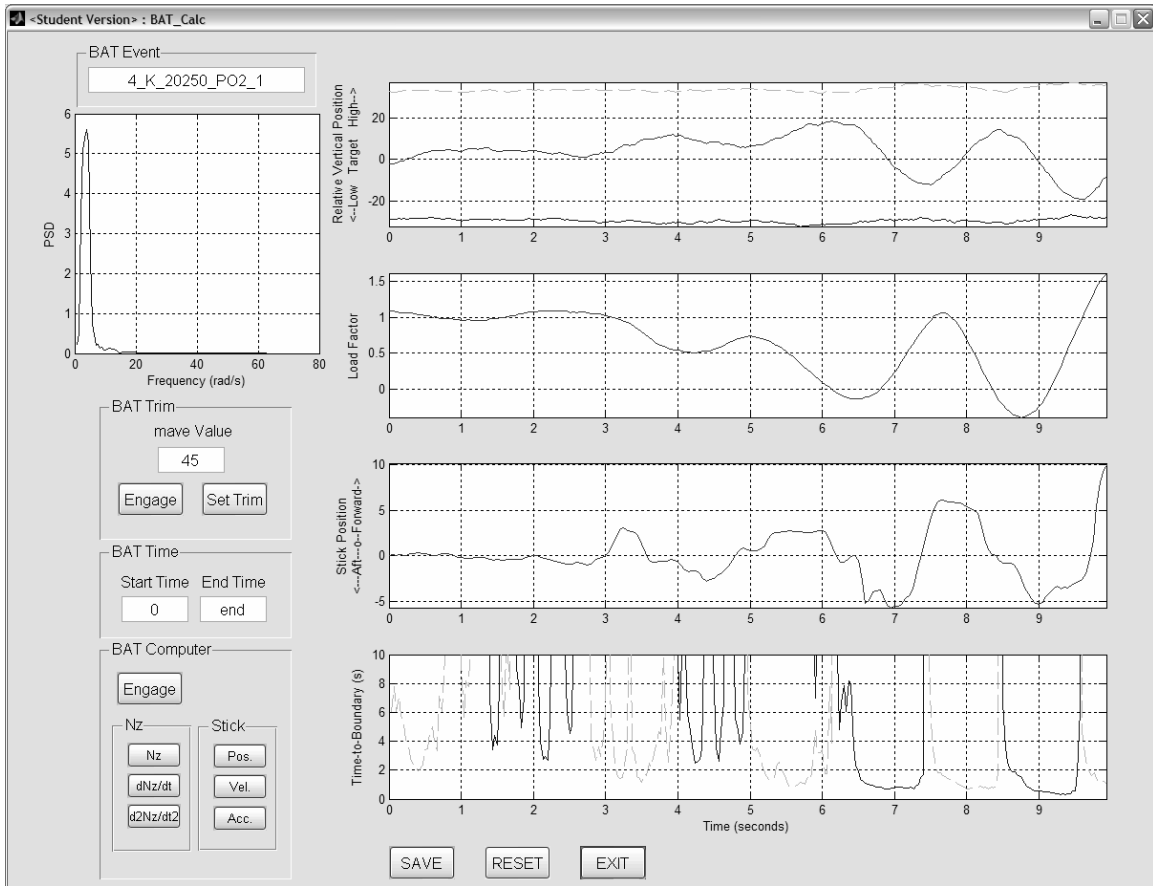


Figure 15. BAT Data Analysis Tool – BAT_Calc

BAT_Calc provided four primary functions: estimation of longitudinal stick trim position, estimation of pilot actuation frequency, calculation of distance to boundary from visual data, and collation of visual and DAS data. This section will focus on the calculation of distance to boundary from visual data and the collation of visual and DAS data. Estimation of longitudinal stick trim position and determination of pilot actuation frequency will be discussed in subsequent sections.

The visual data provided by the ScratchClick tool provided the pixel positions of the boundaries, the wingtip, and the center of the chevron star. Two points each were used to define the upper and lower boundaries, one point for the wingtip, and one point for the center of the chevron star. Figure 16 details how the points were selected in ScratchClick and how they are referenced in the BAT_Calc GUI.

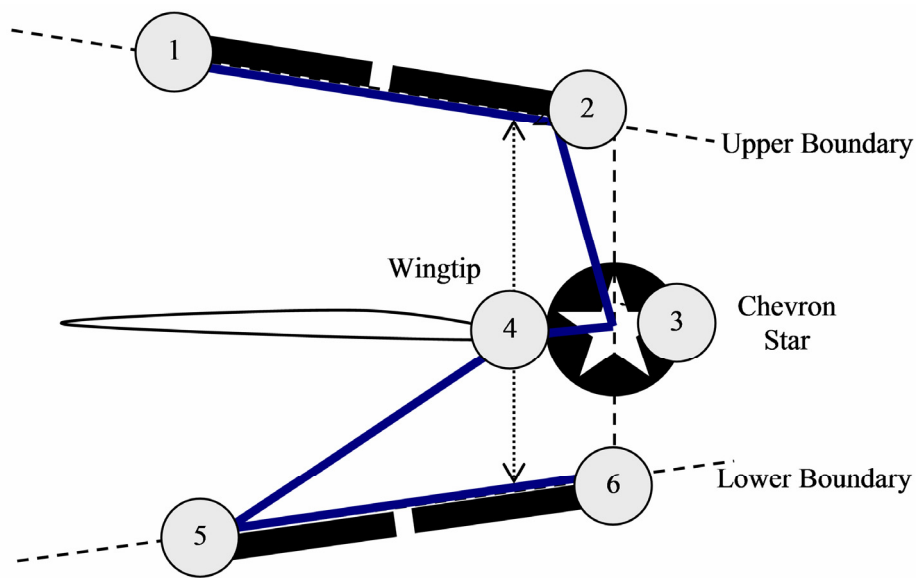


Figure 16. Schematic of Visual Data Point Selection

Points 1 and 2 were used to determine the equation of the line that defined the upper boundary; likewise, points 5 and 6 were used for the lower boundary. Point 3, the center of the chevron star, was used as the center point of the tracking task. The x-coordinate of point 3 was used to draw a vertical line that intersected both the upper and

lower boundaries. Those points of intersection then defined the pixel distance of each boundary from the center of the tracking task.

The wingtip, point 4, was assumed to track along the vertical line calculated from point 3 throughout the event. The distance from the tracking task center point was simply the difference in y-coordinate values between points 3 and 4. The following equations detail the algorithm described above. The subscripts of each x and y variable reference the points as shown on Figure 16.

$$\begin{aligned}
 m_{upper} &= \frac{y_2 - y_1}{x_2 - x_1} \\
 m_{lower} &= \frac{y_6 - y_5}{x_6 - x_5} \\
 y_{ub} &= m_{upper} * x_3 + (y_1 - m_{upper} * x_1) \\
 y_{lb} &= m_{lower} * x_3 + (y_5 - m_{lower} * x_5) \\
 d_{upper} &= y_3 - y_{ub} \\
 d_{lower} &= y_3 - y_{lb} \\
 d_{wingtip} &= y_3 - y_4
 \end{aligned} \tag{4}$$

Where:

m = the slope of the specified line

y = vertical pixel position of specified point

x = horizontal pixel position of the specified point

d = pixel distance between two pixel positions

Note: pixel positions were numbered from the top left corner of each image; therefore, to produce boundaries about the zero reference point, y_3 , the d_{lower} value was calculated as a negative distance

This algorithm was then applied to each frame of visual data to develop a time history of each event. An example time history is provided in Figure 17, where the

distance to boundary is highlighted. The solid line in the middle of the plot shows the position of the wingtip; the dashed line on the top of the plot shows the lower boundary; and the solid line at the bottom of the plot shows the upper boundary. The position of the boundaries was reversed to better reflect the relative position of the test aircraft. If the wingtip is above zero, then the test aircraft is above the target aircraft and the target aircraft wingtip appears to be closer to the lower boundary, and vice versa. This presentation was more intuitive to the flight crew during the post flight data analysis. With the position information now determined, the time-to-boundary can be calculated.

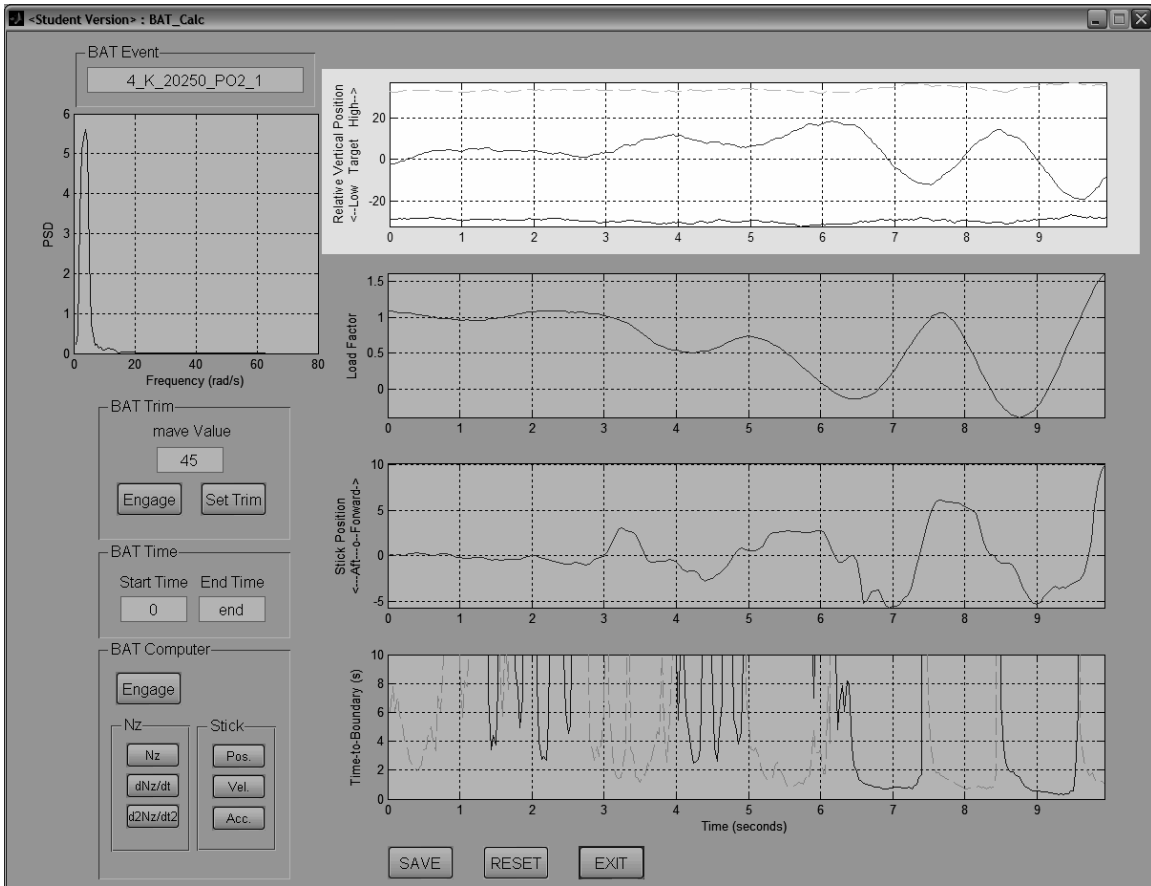


Figure 17. Distance to Boundary Time History – BAT_Calc Display

As shown in equation 2, the time-to-boundary was calculated from both the distance to boundary and the rate to boundary. The distance to boundary was calculated directly from the position information obtained from the position time history. Consequently, the distance to boundary, $D_{boundary}$, for both the upper and lower boundaries was simply determined from the difference in the y-coordinates of the wingtip and the boundaries.

$$\begin{aligned}
D_{upper} &= d_{upper} - d_{wingtip} = y_4 - y_{ub} \\
D_{lower} &= d_{lower} - d_{wingtip} = y_4 - y_{lb}
\end{aligned}
\tag{5}$$

Where:

D_{upper} = pixel distance of target wingtip to upper boundary

D_{lower} = pixel distance of target wingtip to lower boundary

The rate to each boundary was determined through the numerical derivative of the distance to boundary. Hence, the derivative was approximated by:

$$r_{boundary} = \frac{\Delta D_{boundary}}{\Delta t}
\tag{6}$$

Where:

$r_{boundary}$ = rate to boundary

Once both the distance and rate to boundary values were calculated, the time-to-boundary was calculated by dividing the distance to boundary by the rate to boundary. An important note here is that the distance and rate to boundary values were calculated based on pixel distances; that is, the difference between pixel locations on one frame of the visual data. Since the assumption was made that the visual data provided by the aircraft mounted camera system was representative of what the pilot viewed during the BAT events, the pixel distances were assumed to reflect the actual visual distances the pilots were tracking. Therefore, the actual physical distances were not required for the determination of the time-to-boundary. Figure 18 shows a representative plot of the time-to-boundary as displayed in the BAT_Calc GUI. The dashed line references the time to the lower boundary and the solid line the time to the upper boundary.

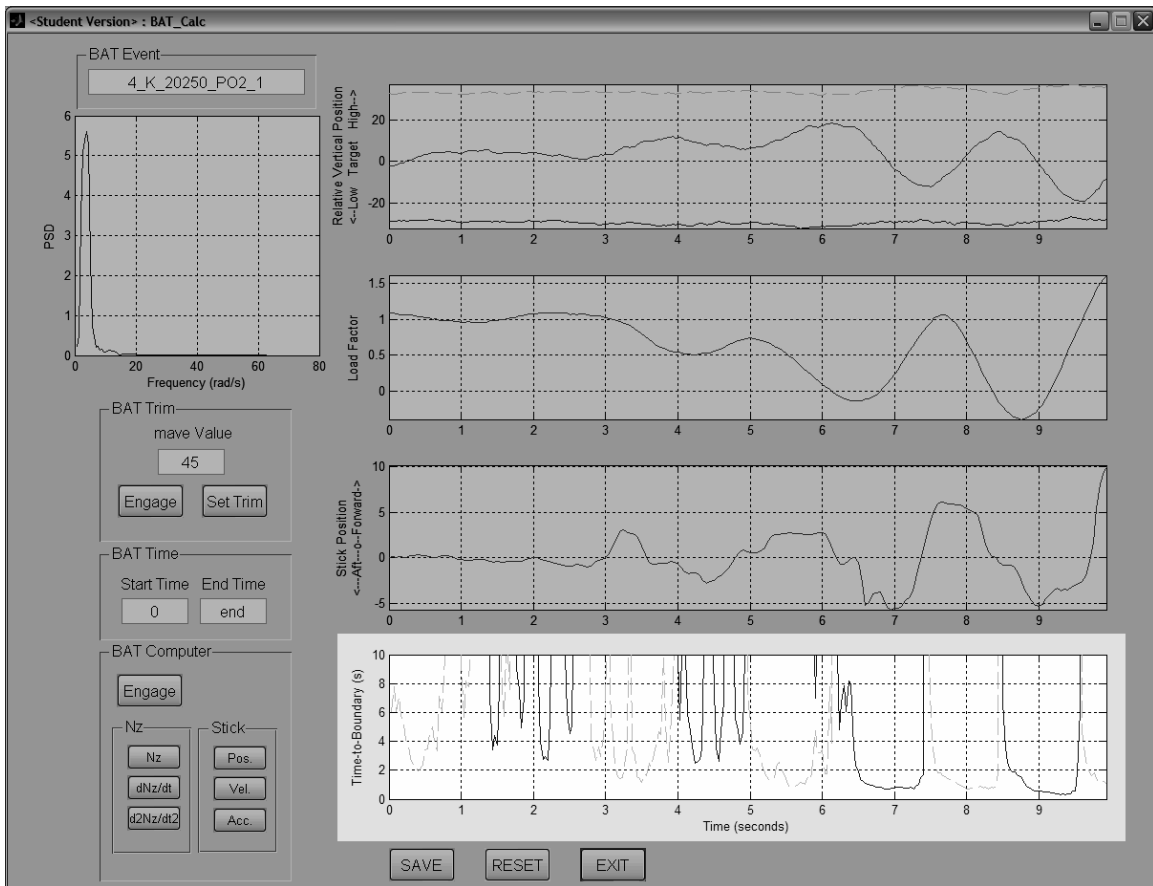


Figure 18. Time to Boundary Time History – BAT_Calc Display

The only remaining parameter required to determine all of the BAT parameters of interest is the longitudinal stick position.

4.4.2 Estimating Longitudinal Stick Trim Position

Pilot system inputs were measured via the longitudinal stick displacement recorded by the aircraft DAS. The stick displacement was measured at a rate of 20 samples per second and had a range of approximately 45 degrees. On the ground the stick was centered at approximately 5 degrees forward stick; however, in flight the stick

was centered about a trim position for each flight condition. The developed flight test techniques also required a rapid change in flight condition leading to time-dependent trim positions. Thus, a method for estimating the stick trim position resulting from rapidly changing flight conditions was required to more accurately present the magnitudes of the pilot inputs.

The BAT_Calc tool utilized a moving point averaging technique developed at the National Aeronautics and Space Administration's Dryden Flight Research Center to estimate the longitudinal stick trim position. This Matlab® function, titled MAVE, averaged the specified number of points before and after the point of interest and repeated this for each point in the specified array. MAVE allowed for the input of the number of points to average around each data point. In the BAT_Calc GUI, this MAVE value was adjusted until a suitable fit to the data was obtained. Figure 19 depicts the plots of both the collected data parameters (solid lines) and the averaged trim histories (dashed lines).

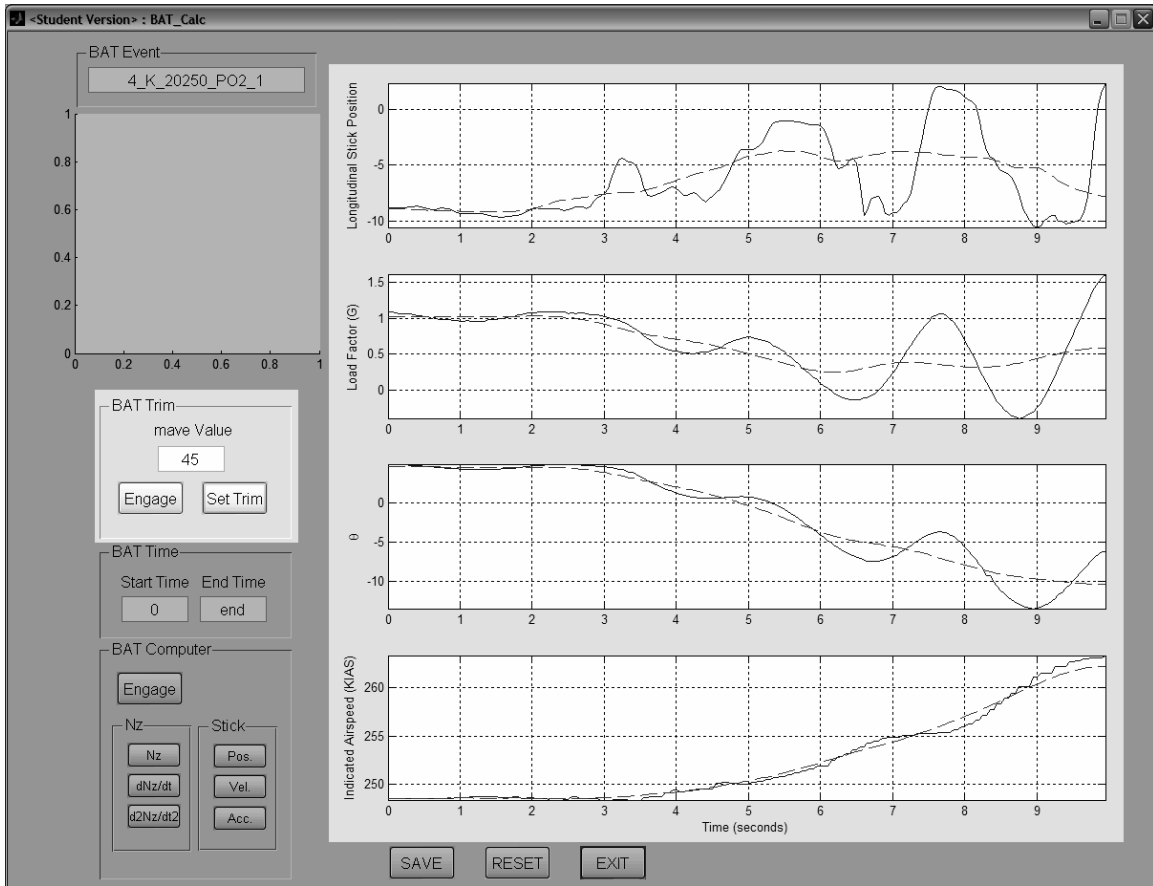


Figure 19. Longitudinal Stick Trim Position - BAT_Calc Display

To aid in establishing a suitable fit, the aircraft airspeed and pitch attitude were used along with the stick position (see Figure 19). In fact, the pitch attitude and the airspeed were used primarily to establish the value of the MAVE function as those two parameters were used by the target aircraft pilots to execute the flight test techniques. Once a satisfactory fit was obtained, the longitudinal stick trim position time history was established. From this point, the longitudinal stick position used for the determination of

the BAT parameters was the difference between the DAS recorded stick position and the estimated trim stick position.

4.4.3 Identification of K_{max} and t_{Kmax}

With the stick trim position estimated and the time histories developed, the identification and determination of the key BAT parameters can be conducted. The easiest BAT parameters to identify in the collected data were the maximum boundary tracking feedback gain, K_{max} , and the time-to-boundary for the maximum boundary tracking feedback gain, t_{Kmax} . K_{max} was simply recorded as the stick deflection from trim at the point when a maximum stick deflection occurred during a BAT event. The t_{Kmax} parameter was then the time to boundary that corresponded to the maximum stick deflection. Figure 20 shows how these two values were taken from the BAT_Calc GUI. Once the maximum longitudinal stick position was identified from the stick position time history, a vertical line was drawn and the time-to-boundary associated with that stick position was recorded as t_{Kmax} . If the stick position data point was between two time-to-boundary data points, then linear interpolation was used to determine the time-to-boundary.

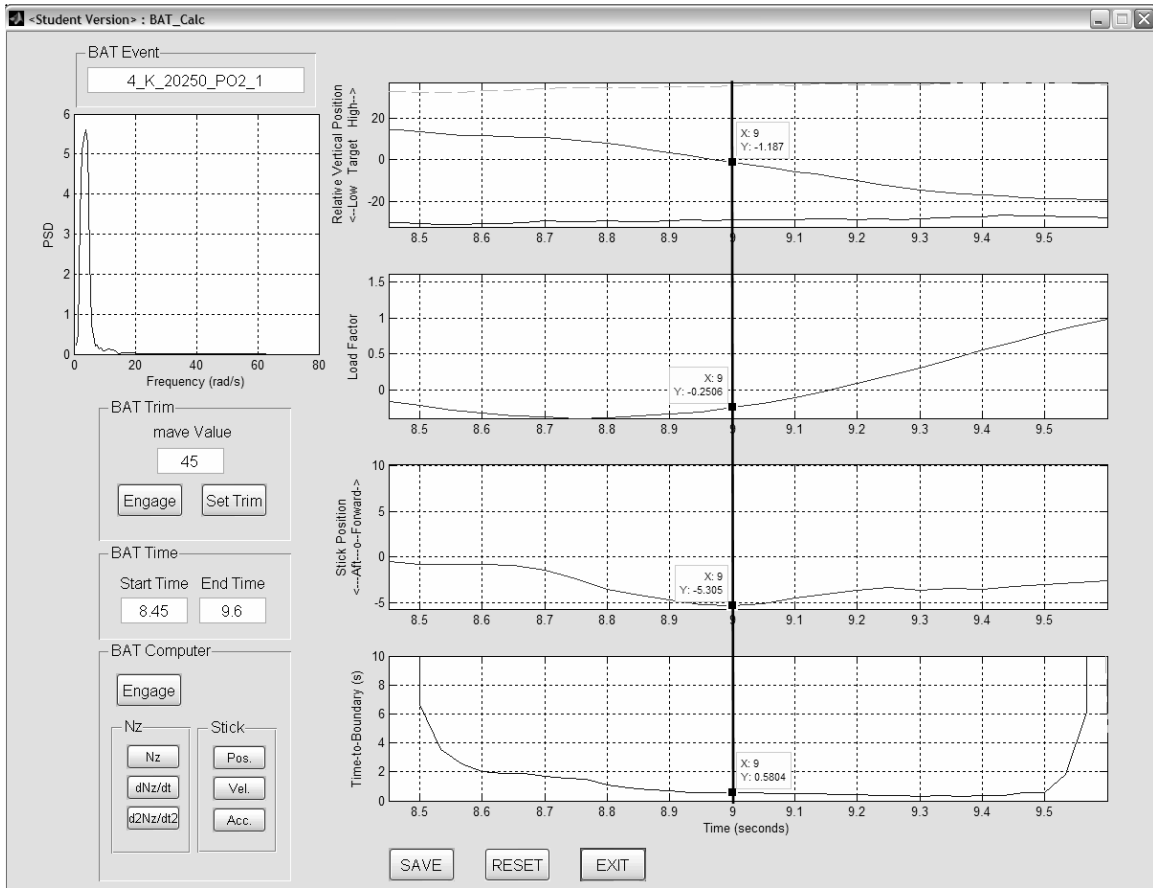


Figure 20. Determination of K_{max} and t_{Kmax} - Bat_Calc Display

It's important to note that the value of K_{max} , as defined in equation 2, corresponds to a gain value used to model the BAT feedback loop. The K_{max} determined from the flight test data is not a direct analogy to the K_{max} originally defined by Mr. Gray. To determine the analogous value of K_{max} , the BAT model should be fitted to the flight test data. That was not accomplished during this experiment and is an area that can be investigated in the future. Nonetheless, the values of the maximum stick deflections and

the associated times-to-boundary were determined as shown in Figure 20 and are summarized in the Appendix.

4.4.4 Determination of t_{Kmin}

The time-to-boundary for minimum boundary tracking feedback gain, or t_{Kmin} , proved to be the most difficult parameter to identify. Originally it was theorized that a definitive event in stick position (such as a flattening or rapid reversal) would provide the cue for the determination of the t_{Kmin} . However, that distinctive event was never apparent in any data set. A method had to be developed that would allow for the determination of this key parameter.

Methods involving stick velocity, stick acceleration, load factor, and rate of change of load factor were investigated as potential cues for t_{Kmin} . The acceleration of the longitudinal stick position proved to be repeatable and reliable at providing a time-to-boundary at which a BAT event began. This method correlated a large stick acceleration in the direction of the boundary with a time-to-boundary greater than t_{Kmax} .

The stick acceleration is a direct indicator of the pilot's applied force. Since pilots apply forces to control inceptors in order to obtain desired inceptor positions and therefore desired aircraft responses, stick force is a good indication of pilot intent. Therefore, looking at the point where the pilot's applied stick force made a sharp increase opposite the approaching boundary was a good indication of the point at which the pilot first attempted to avoid the boundary.

The stick acceleration was calculated by differentiating the stick position data twice. It was then plotted in the BAT_Calc GUI for determination of t_{Kmin} . Figure 21

depicts the same BAT event as that pictured in Figure 20. However, the stick position has been replaced with the stick acceleration. Here the pilot applies an aft stick force as the aircraft begins to descend relative to the target aircraft in an effort to arrest the closure to the impending boundary.

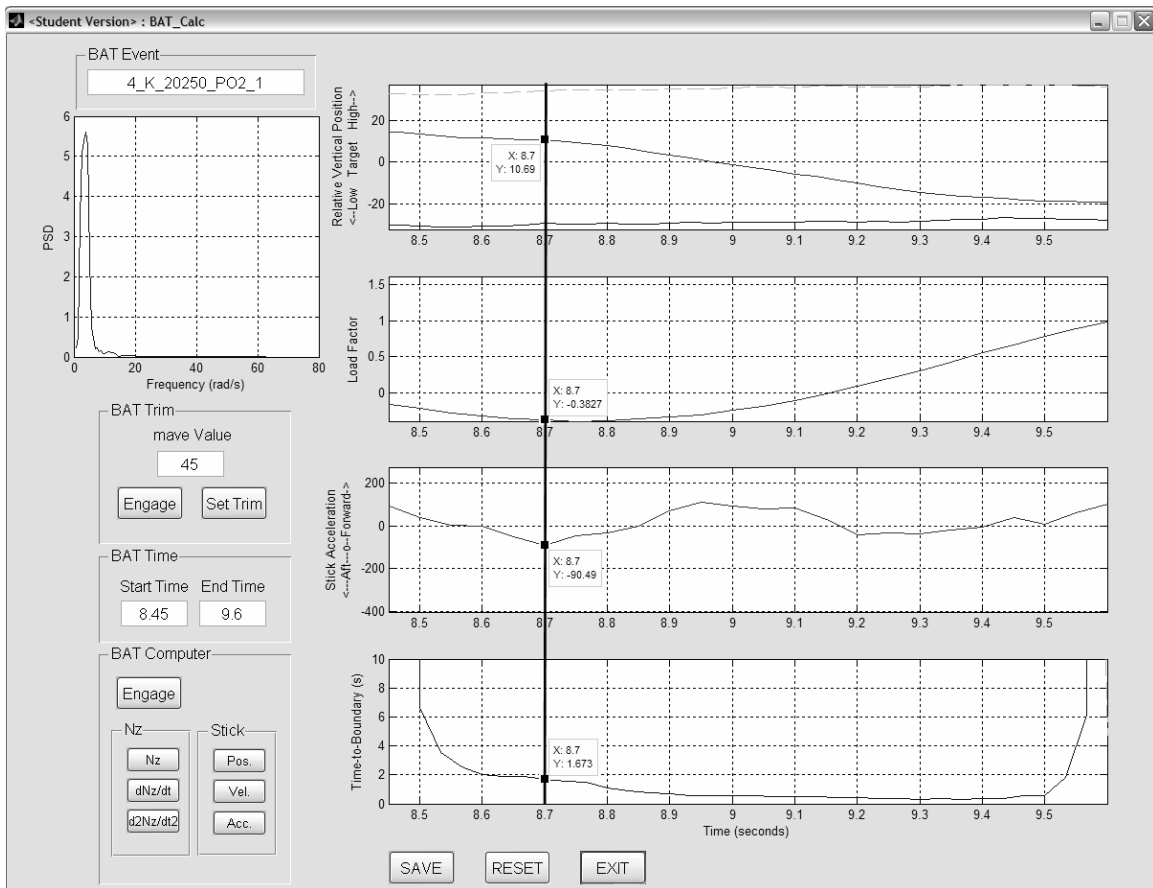


Figure 21. Determination of t_{Kmin} - BAT_Calc Display

Two important notes resulted from the determination of t_{Kmin} . The first was that there appeared to be a learning curve during the BAT events. With events that had

multiple boundary avoidance occurrences, the t_{Kmin} values associated with each occurrence generally decreased in value as the events progressed. This is potentially important as t_{Kmin} may be defined by the very first occurrence of boundary avoidance tracking and not independently at each occurrence during a BAT event. If this is true, much more data will have to be analyzed to characterize t_{Kmin} and its relationship with other parameters. The values of t_{Kmin} determined and presented in Appendix A are the values associated with each occurrence of each BAT event.

The second note is that in some of the data the times-to-boundary appeared to be affected by the aircraft load factor. To evaluate this relationship, the load factor at the point of boundary awareness was recorded during the data reduction as well. The analysis of this relationship will be presented in section 4.4.6.

4.4.5 Pilot Actuation Frequency Determination

To investigate the proximity of the system operating frequency to the system crossover frequency, determination of the frequency at which the pilot was providing inputs to the system was required. To calculate this parameter, a power spectral density (PSD) was performed on the longitudinal stick position data. The determined pilot actuation frequency was assumed constant for the duration of the BAT event; consequently, regardless of the number of occurrences within a single event, the pilot actuation frequency was the same.

The applied technique for the determination of the PSD was a Matlab[®] function again obtained from NASA DFRC. The function utilized the Matlab[®] built-in fast Fourier transform function, FFT, to calculate the frequency domain information of the

longitudinal stick position. Once the data were converted to the frequency domain, the function then computed the amplitude by first multiplying the FFT output amplitude by its complex conjugate and dividing the result by the number of data points. Then the data was smoothed by the MAVE function using a 5 point average. Finally, since the Fourier transform calculated the amplitude data as symmetric about zero frequency, half of the data was then multiplied by the time differential to compute the PSD of the longitudinal stick position time history. The resulting plot from this algorithm was then displayed on the BAT_Calc GUI allowing the user to determine the pilot actuation frequency (see Figure 22). The pilot actuation frequencies for each analyzed event are located in the Appendix.

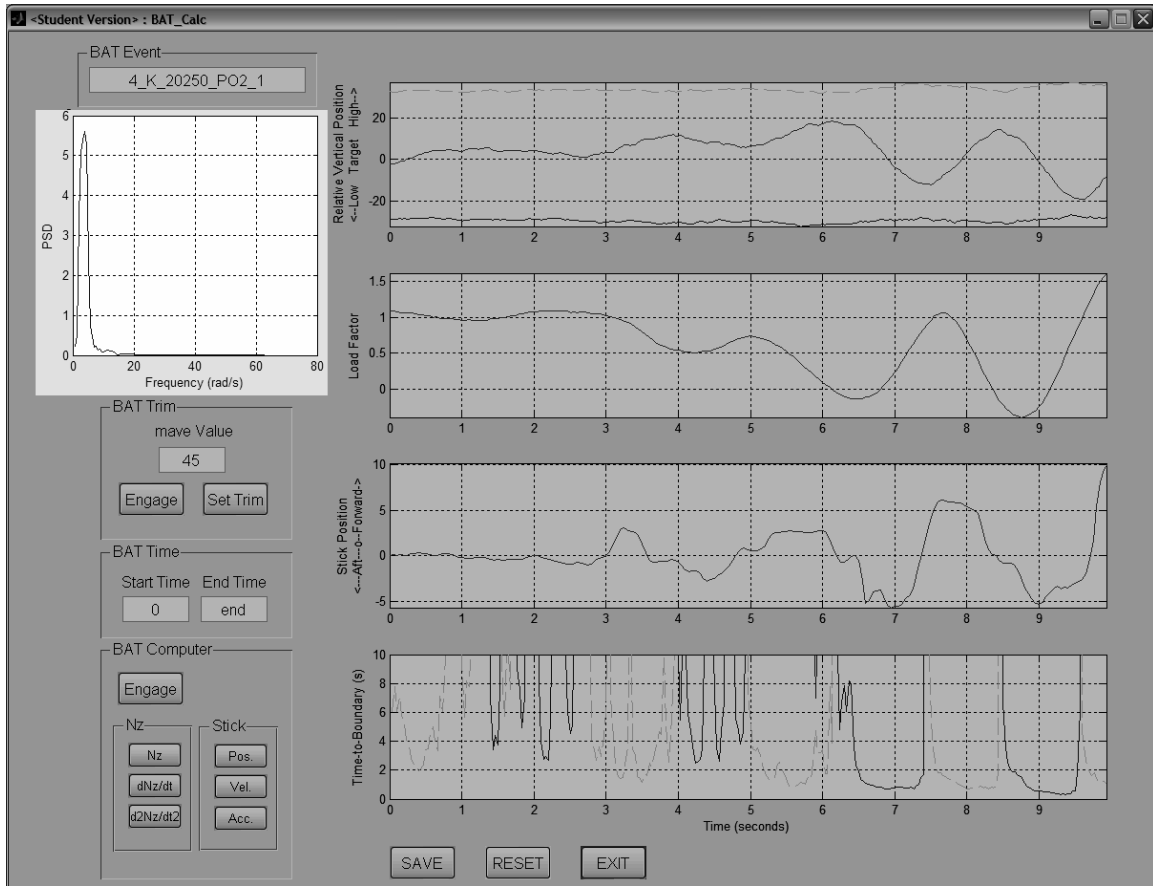


Figure 22. PSD of Longitudinal Stick Position - BAT_Calc Display

4.4.6 Analysis of BAT Parameters

Analysis of the BAT parameters of interest, t_{Kmin} , t_{Kmax} , and K_{max} , started with statistical analyses of each parameter. Parameter mean, variance, and 95% confidence interval on the mean were considered during the analyses.

4.4.6.1 Time to Boundary for Minimum Boundary Feedback Gain (t_{Kmin})

The first parameter analyzed was t_{Kmin} . First, all the data collected from the BAT_Calc tool were analyzed to determine if t_{Kmin} possessed a central tendency and to

compare that value to the results of Mr. Gray’s simulator study. Statistical analysis for a total of 36 data points showed that no central tendency existed. Furthermore, the 95% confidence interval on the mean was only 0.78, or 22% confident that the calculated mean was representative of the data set.

Each boundary avoidance occurrence required the aircrew to either increase load factor (pull) or decrease load factor (push) to avoid the impending boundary. The values collected for t_{Kmin} were also divided into “push” and “pull” categories to determine if t_{Kmin} exhibited a central tendency when either the load factor was increasing or decreasing. The results again indicated no central tendency in either push or pull. Table 6 presents the results of the statistical analyses.

Table 6. Results of Statistical Analyses for t_{Kmin}

	t_{Kmin} (all points)	t_{Kmin} (pull)	t_{Kmin} (push)
Mean	3.44	2.14	4.17
Standard Deviation	2.31	0.91	2.54
Sample Variance	5.34	0.84	6.48
Count	36	13	23
95% Confidence	0.78	0.55	1.10

The inconclusive results of the statistical analyses of t_{Kmin} required looking at possible relationships between this and other cueing parameters. Based on the observations made during the determination of t_{Kmin} (section 4.4.4) that time-to-boundary seemed to vary with load factor, this was the relationship that was investigated. The load

factor and rate of change of the load factor at each t_{Kmin} point was collected utilizing the BAT_Calc GUI.

The nuisance parameter study conducted in 2001 provided a time to boundary of approximately two seconds for pilots to begin feeling nervous about the approach to the ground (Prosser, 2001:11). Interestingly, that study seemed to indicate a somewhat constant time to boundary for the specific scenario they established. That number correlates well with Mr. Gray's simulator results of approximately 2.8 seconds (Gray, 2005:11). However, neither study investigated the effect of load factor on the pilot's perception of time to boundary.

4.4.6.2 Correlating t_{Kmin} and Load Factor

To determine if a relationship existed, t_{Kmin} was plotted against both the load factor at t_{Kmin} , G_{Kmin} , the rate of change of load factor at t_{Kmin} , $(\Delta G/\Delta t)_{Kmin}$, as well as variations of the products and quotients of these parameters. First, simply plotting t_{Kmin} and G_{Kmin} against each yielded the results shown in the Figure 23.

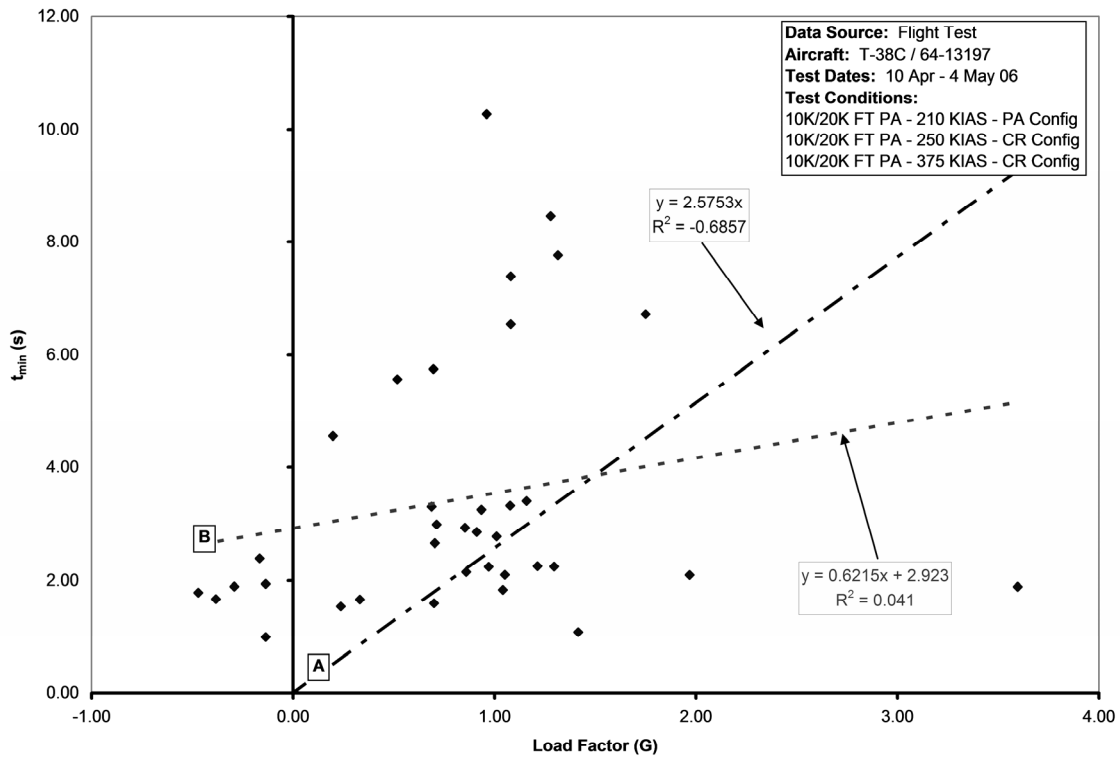


Figure 23. Correlation of t_{Kmin} and G_{Kmin}

The plot shows a wide scatter in the values of t_{Kmin} with respect to the load factor at which t_{Kmin} occurred. A linear regression was performed (line B) and provided a poor R-squared value indicating a poor fit of the data. However, this linear model compared somewhat favorably with results of Mr. Gray’s simulator study. Mr. Gray’s fixed-based simulator provided average results of 2.8 ± 0.25 seconds for t_{Kmin} (Gray, 2005:11). Using the above equation for the linear model and applying a load factor of one resulted in a t_{Kmin} value of 3.54 seconds. With only a 20% difference between the two values, Mr. Gray’s results seem to be relatively close to what was seen during the flight tests.

During the investigation of the many G_{Kmin} and t_{Kmin} combinations, only one other relationship showed any degree of correlation. This relationship, shown in Figure 24, was developed by normalizing both G_{Kmin} and t_{Kmin} by the rate of change of the load factor, $(\Delta G/\Delta t)_{Kmin}$. $(\Delta G/\Delta t)_{Kmin}$ was selected as a parameter of interest for characterizing BAT events because pilots typically respond not just to load factor, but also to how quickly the load factor is changing. A linear regression of the data provided for a much better curve fit than that obtained with the previous relationship.

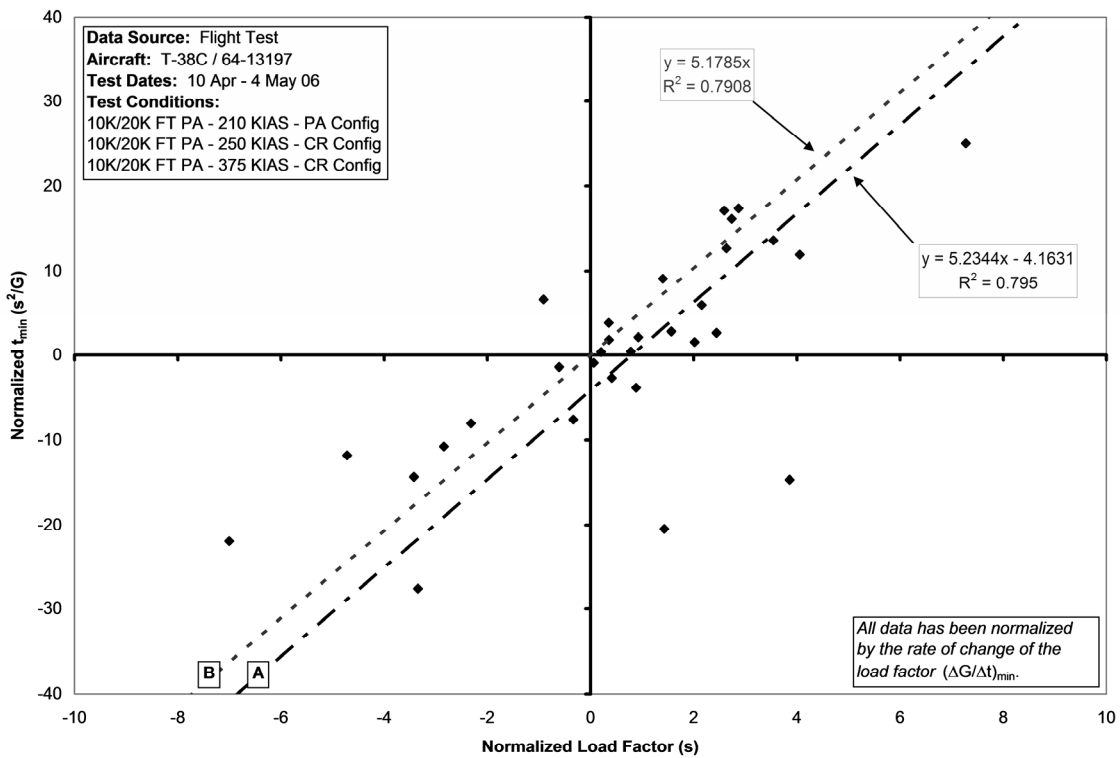


Figure 24. Correlation of Normalized t_{Kmin} and G_{Kmin}

Constraining the linear regression to a zero y-intercept provided for a minor difference in the quality of the curve fit, as shown in the Figure 24 (lines A and B). Therefore, regression B was used for comparison as it simplified the relationship to a constant without greatly affecting the relationship to the collected data. The result provided for the following relationship:

$$\frac{t_{\min}}{\left(\frac{\Delta G}{\Delta t}\right)} = B * \frac{G_{\min}}{\left(\frac{\Delta G}{\Delta t}\right)} \Rightarrow \frac{t_{\min}}{\left(\frac{\Delta G}{\Delta t}\right)} / \frac{G_{\min}}{\left(\frac{\Delta G}{\Delta t}\right)} = B \Rightarrow \frac{t_{\min}}{G_{\min}} = B \quad (7)$$

Where:

$B = 5.18$ (constant determined from the linear regression)

Applying this simplified relationship to the case of a load factor of one resulted in a t_{Kmin} value of 5.18 seconds. Unlike the previous linear regression results, this result did not correlate well with the average t_{Kmin} value obtained from Mr. Gray's simulator study.

Going back to the original investigation comparing t_{Kmin} and G_{Kmin} directly and applying the same zero y-intercept linear regression resulted in an even poorer curve fit (Figure 23, line A). However, for a load factor of one, the t_{Kmin} parameter was 2.57 seconds which again compared favorably with the results of Mr. Gray's simulator study. While the direct comparison results seem to correlate relatively well with Mr. Gray's simulator study results, they do not correlate well with the relationship developed using the normalized parameters, which appears to be more representative of the collected data.

To conclude this investigation, statistical analyses of the ratio of G_{Kmin} to t_{Kmin} were conducted to determine if a central tendency existed in the relationship. If a strong central tendency existed, then the theory of a constant that describes the relationship between t_{Kmin} and load factor would be strengthened. Performing the same analyses as for the original t_{Kmin} investigation provided the results shown in table 7.

Table 7. Statistical Analyses of the Ratio of G_{Kmin} to t_{Kmin}

	G_{Kmin}/t_{Kmin}	$ G_{Kmin} / t_{Kmin} $	$(G_{Kmin} / t_{Kmin}) / (\Delta G/\Delta t)_{Kmin}$
Mean	0.30	0.35	0.47
Standard Deviation	0.40	0.36	0.40
Sample Variance	0.16	0.13	0.16
Count	36	36	36
95% Confidence	0.13	0.12	0.14

From these analyses it is clear that there is a relationship between the time to boundary for minimum boundary tracking feedback gain and the load factor at the time of boundary awareness. The exact nature of the relationship stills bears some investigation, but as a first order approximation to this relationship, the author suggests:

$$\frac{t_{min}}{G_{min}} = 5.18 \quad (8)$$

This relationship provides for the best representation of the collected data and best represents what was experienced while in flight.

4.4.6.3 Time to Boundary for Maximum Boundary Feedback Gain (t_{Kmax})

The next parameter analyzed was t_{Kmax} . The same statistical analyses were performed on the collected values of t_{Kmax} as those performed on t_{Kmin} ; however, very different results were obtained. The analysis indicated that t_{Kmax} was an independent parameter. The data exhibited a fairly strong central tendency with a mean value of 0.78 ± 0.18 seconds. The 95% confidence interval was 0.14 or 86% confident that the mean was representative of the data set.

Again similar to the analysis for t_{Kmin} , the t_{Kmax} data points were divided into pull and push categories to determine if there was a variation in t_{Kmax} based on increasing or decreasing load factor. As shown in the table 8, the analysis shows a small difference between the values. This difference is within the variance of the mean for all of the collected data; furthermore, when the total number of data points is split into two separate categories, the number of data points in each category is too small to provide a statistically significant solution. Therefore, based on the data available, there is no appreciable difference in time to boundary for maximum boundary tracking feedback gain (t_{Kmax}) between increasing or decreasing load factors. In summary, it appears that t_{Kmax} is a constant value for all pilots at all flight conditions evaluated in this experiment.

Table 8. Statistical Analyses of $t_{K_{max}}$

	$t_{K_{max}}$ (all points)	$t_{K_{max}}$ (pull)	$t_{K_{max}}$ (push)
Mean	0.78	0.82	0.75
Standard Deviation	0.42	0.44	0.41
Sample Variance	0.18	0.20	0.17
Count	34	13	21
95% Confidence	0.14	0.27	0.19

4.4.6.4 Maximum Boundary Feedback Gain (K_{max})

The final BAT parameter to be determined was the maximum boundary tracking feedback gain. As stated previously, this gain was assumed to be proportional to the longitudinal stick position. The results of the analysis of the longitudinal stick position were assumed to provide a representative solution of the actual K_{max} parameter.

Applying the same type of statistical analyses to the longitudinal stick position data as applied to both $t_{K_{min}}$ and $t_{K_{max}}$ yielded inconclusive results. The stick positions at both $t_{K_{min}}$ and $t_{K_{max}}$ were evaluated as well as the difference between the two parameters. The parameters were also divided up into push and pull categories with similarly inconclusive results. Table 9 lists the results of the statistical analyses.

Table 9. Statistical Analyses of Boundary Feedback Gain

	K_{min}	K_{min} (pull)	K_{min} (push)	K_{max}	K_{max} (pull)	K_{max} (push)	ΔK	ΔK (pull)	ΔK (push)
Mean	0.24	0.01	0.37	0.66	-4.45	3.83	0.32	3.28	-4.46
Standard Deviation	2.33	2.15	2.46	4.72	2.54	2.34	4.60	2.35	2.99
Sample Variance	5.43	4.62	6.08	22.31	6.44	5.47	21.15	5.51	8.97
Count	36	13	23	34	13	21	34	21	13
95% Confidence	0.76	1.17	1.01	1.59	1.38	1.00	1.55	1.00	1.63

Unfortunately this parameter is not as straightforward as a pilot's perceived time to boundary. The magnitude of the longitudinal stick deflection is a function of the pilot's threat perception and comfort level. As stated in Chapter 3, the pilots in this experiment attempted to role play the tracking task by treating the boundaries as hazardous. This was an attempt to allow the pilots to use the maximum longitudinal stick deflection possible. In contrast, in all of the data analyzed, no pilot ever reached the maximum allowable stick deflection during any tracking task. This indicates that the pilots were self-limiting the magnitude of their stick inputs to prevent an uncomfortable situation. This self-limiting confounded the results of the analyses of the stick deflection with each pilot.

4.4.6.5 Time Between t_{Kmin} and t_{Kmax}

In addition to all of the collected parameters, the time from the first BAT input to the maximum BAT input, Δt , was recorded for each BAT occurrence. This parameter was intended to be used in the development of characteristic and non-dimensional BAT parameters; however, when a statistical analysis was performed on this parameter, a surprising result was obtained. It was found that the data exhibited a strong central tendency, indicating that this time differential was fairly consistent among all pilots and flight conditions.

The value of this parameter was determined to be 0.55 ± 0.13 seconds. With the typical variability in the time delay inherent in each pilot and the difference in aircraft time delay with each flight condition, the fact that this parameter exhibited some independence was indeed surprising. This result potentially points to another intrinsic

human characteristic; that once an individual recognizes a hazardous situation, they will instinctively use their maximum effort to avoid the situation within 0.55 ± 0.13 seconds.

4.5 Correlation of Flying Qualities and Boundary Avoidance Tracking

After determination of the BAT and flying qualities parameters, the final step was to investigate the relationship between the two sets of parameters. All of the BAT parameters were plotted against each of the flying qualities parameters to determine if any correlation existed. To limit the dispersion of the collected data about each flight condition, the average values of each parameter at each flight condition were used for this analysis.

Only one potential correlation between the BAT parameters and aircraft flying qualities was evident from the collected data. Figure 25 shows the relationship between G_{Kmin}/t_{Kmin} and the system crossover frequency, ω_{180} .

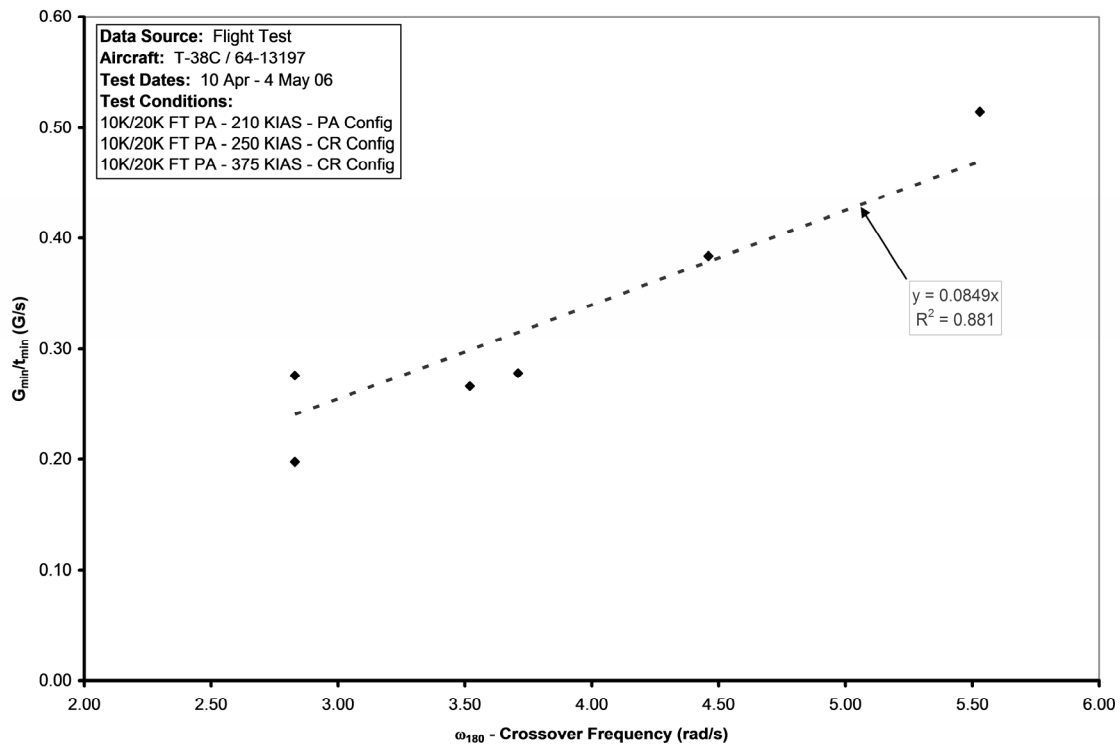


Figure 25. Correlation of G_{Kmin}/t_{Kmin} with System Crossover Frequency

While this relationship presents a possible correlation between BAT and flying qualities, further analysis is required before this relationship can be solidified. Since the BAT parameters were averaged for each flight condition, the number of data points at each flight condition was very small, between only two and ten. With such small sample populations, the average values are very likely not representative. Also, the applied technique for the determination of the system crossover frequency did not provide a high level of confidence in the determined values.

Most importantly, what this correlation shows is that the factors that characterize pilot boundary awareness in the dynamic flight environment are extremely complex.

While t_{Kmax} appears to be an intrinsic human characteristic, t_{Kmin} is at minimum a function of both load factor and a characteristic system frequency.

In addition to the graphical correlation just discussed, one other relationship was determined through statistical analyses. The ratio of the pilot actuation frequency, ω_{BAT} , to the system crossover frequency, ω_{180} , was found to have a very strong central tendency. The ratio was found to be 1.12 ± 0.06 with a 95% confidence level of 0.08. This result seems to indicate that the pilots operated very close to the system crossover frequency.

However, the size of the data population for this analysis was small and the same low confidence crossover frequency data were used in the analysis. As referenced previously, the pilot actuation frequency was assumed to be constant through each BAT event. A total of 12 events and 36 occurrences were evaluated and the determined pilot actuation frequencies were assumed constant throughout each event; so, only 12 different values for ω_{BAT} were calculated and compared with six values of ω_{180} . Therefore, further data reduction is required to make a more conclusive statement about this relationship. Preliminarily though, this result may help explain the divergent oscillations experienced by the aircrews.

4.6 Aircrew Comments

4.6.1 Flying Qualities Effects

During execution of the flight testing, all pilots noted that a particular flight condition appeared to produce more oscillatory BAT events than the others. Though this flight condition was different for each pilot, these initial observations seemed to provide

some support for the theory of flying qualities dependence of the BAT parameters. Unfortunately the data analyzed here does not support this assumption. The data were, however, extremely limited in the aircraft flying qualities parameters with only two parameters evaluated. It is possible that a correlation does exist, but further analyses including several other aircraft flying quality parameters needs to be accomplished.

4.6.2 PIOs Resulting From Repeated Boundary Avoidance Tracking Events

All pilots described the rapid oscillatory motion of repeated BAT occurrences as PIOs. While attempting to avoid the opposing boundaries, the pilots experienced a sense of uncontrollability of the aircraft. They applied the PIO recovery techniques of freezing or releasing the controls once a boundary excursion occurred. The boundaries obviously acted to increase the pilots' gains during the tracking tasks and potentially drove them close to the system crossover frequency rendering the pilot's-eye system unstable.

5. Discussion

5.1 Summary of Findings

Overall, this experiment showed that the presence of boundaries can provide a destabilizing influence and hinder a pilot's ability to successfully accomplish a specified task. Through the use of two T-38 aircraft, a video camera system, and specially developed flight test techniques, BAT was elicited over several different flight conditions and a sizable amount of data generated. Analysis of a portion of that data has provided much more insight into the parameters that currently define BAT.

The data supports what appears to be an intrinsic human characteristic for perception of hazard avoidance. The perceived time to boundary when an individual will make their strongest attempt to avoid an approaching hazard is 0.78 ± 0.18 seconds. The time to boundary for boundary awareness appears to be a function of at least load factor and possibly a characteristic system frequency. As a first approximation, the ratio of load factor to time to boundary for boundary awareness is 0.35 ± 0.13 . Finally, the amount of time it takes for a pilot to go from boundary awareness to maximum control input is 0.55 ± 0.13 seconds. Again this appears to be characteristic of the human perception of hazards. This information will help to improve the current models of BAT and may eventually lead to more robust human-in-the-loop control systems

For the flight test community, this experiment developed flight test techniques that are readily adaptable to any flight test project that may be conducting handling qualities investigations. The use of boundaries is a method that can help increase pilot gains when investigating system instabilities. More importantly, though, is

understanding the effect that placing boundaries has on the ability of a pilot to successfully conduct a specified task.

5.2 Lessons Learned

Use of a camera system to capture the pilot's perspective was key to more fully characterizing BAT. Since the pilot is an integral part of the whole system, the more closely the data is associated with the actual pilot stimuli, the better the characterization of the BAT parameters. However, there is a cost associated with this level of fidelity.

While the camera system provided the perspective needed, the ability to obtain the necessary information from the recorded video images must be more fully developed for this type of experimentation and testing to be beneficial. The extraction of the data from the video information must be automated due to the large amount of data contained within a single frame of video. Additionally, to aid the automation routine, a high-resolution, and possibly high-speed, camera system must be employed. The data collected during this experiment is excellent quality; however, the lack of a functional automated routine prevented examination of more than 70% of the collected data.

5.3 Recommendations for Future Research

Continued investigations of the relationship between aircraft flying qualities and BAT parameters are necessary to further characterize this tracking mode. Aircrew comments from this experiment suggest that a potential relationship exists; thus, determining what that relationship is from the numerous flying qualities parameters will help shed much more light on this new perception of tracking.

Additionally, finding a relation between the time-to-boundary for boundary awareness and other cueing parameters (such as load factor or pitch rate) will help to better characterize the point at which the pilot switches to boundary avoidance. While a technique was developed to help identify this transition point, a relation that includes more pilot cueing parameters will ultimately lead to a more accurate depiction of the transition.

Appendix – Collected Data

#	P	Alt ft	A/S KIAS	Gear	Event	Bound	Motion	Min Gain Time-to-Boundary			Max Gain Time-to-Boundary								
								t_{start} sec	t_{end} rad/sec	ω_{pitch} rad/sec	f_{min} sec	K deg	G G/sec	$(\Delta G/\Delta t)$ G/sec	f_{max} sec	Δt sec	K _{lim} deg	G G/sec	$(\Delta G/\Delta t)$ G/sec
2	K	10K	210	Down	PO	Dashed	Push	2.00	4.00	3.770	3.25	2.23	0.93	-0.40	0.65	1.15	2.31	0.15	-0.51
9	H	10K	210	Down	PO	Dashed	Push	3.50	5.00	3.770	2.99	4.48	0.71	-0.21	1.10	0.15	5.78	0.68	-0.38
9	H	10K	210	Down	PO	Dashed	Pull	4.80	6.20	3.770	1.54	-5.68	0.24	0.17	1.36	0.15	-7.92	0.30	0.47
9	H	10K	210	Down	PO	Dashed	Push	6.00	8.00	3.770	2.10	6.65	1.05	-0.10	1.03	0.15	8.59	0.98	-0.55
9	H	10K	210	Down	PO	Dashed	Pull	7.50	9.50	3.770	1.67	1.17	0.33	0.93	0.37	1.15	-8.55	0.46	0.72
9	H	10K	250	Up	PO	Dashed	Push	3.00	5.00	3.770	2.86	-0.71	0.91	-0.13	1.11	0.55	3.07	0.74	-0.56
9	H	10K	250	Up	PO	Dashed	Pull	6.50	7.80	3.770	4.55	-0.97	0.20	-0.60	1.10	0.60	-4.05	0.36	0.85
9	H	10K	250	Up	PO	Dashed	Push	7.70	9.00	3.770	2.94	0.39	0.85	0.12	0.85	0.65	4.03	0.41	-1.17
9	H	10K	250	Up	PO	Dashed	Pull	8.80	10.00	3.770	0.99	1.11	-0.14	0.15	0.62	0.40	-7.05	0.28	2.02
6	H	10K	375	Up	PO	Circle	Push	2.00	3.20	7.069	7.76	-0.26	1.32	0.48	0.36	0.35	2.13	1.31	-0.65
1	M	10K	375	Up	PO	Solid	Push	3.00	4.50	4.712	5.57	-0.44	0.52	-0.03	1.27	0.70	2.44	1.00	0.53
6	H	10K	375	Up	PO	Circle	Push	3.50	4.30	7.069	8.45	0.74	1.28	0.49	0.27	0.45	1.01	1.07	-0.86
4	K	10K	375	Up	PO	Dashed	Push	3.60	4.80	4.937	5.75	-1.49	0.70	-0.21	0.50	0.45	2.16	0.83	-0.18
6	H	10K	375	Up	PO	Circle	Pull	4.20	5.40	7.069	2.15	-0.12	0.86	-0.18	0.83	0.70	-1.53	1.19	1.32
6	H	10K	375	Up	PO	Circle	Push	5.30	6.00	7.069	1.08	-2.04	1.42	0.70	0.08	0.40	3.65	1.42	-1.36
4	K	10K	375	Up	PO	Dashed	Pull	11.40	12.40	4.937	1.60	2.31	0.70	0.76	0.37	0.30	-4.65	0.85	1.26
7	K	20K	210	Down	PO	Dashed	Push	2.00	4.00	4.189	3.32	-0.81	1.08	0.03	0.80	0.60	2.94	0.95	-0.53
7	K	20K	210	Down	PO	Dashed	Push	7.20	8.90	4.189	3.30	-1.79	0.69	0.26					
2	K	20K	250	Up	PO	Dashed	Push	3.00	5.00	3.59	7.39	-1.31	1.08	0.03					
6	H	20K	250	Up	PU	Dashed	Pull	4.00	6.40	3.77	2.26	1.16	1.21	-0.09	1.21	0.75	-2.39	0.71	1.04
4	K	20K	250	Up	PO	Dashed	Push	4.80	6.40	3.77	2.66	0.76	0.70	-0.25	0.89	0.40	2.77	0.48	-0.80
2	K	20K	250	Up	PO	Dashed	Pull	5.50	6.80	3.59	1.90	2.34	-0.29	-0.70	0.13	0.60	-5.68	0.42	2.71
6	H	20K	250	Up	PU	Dashed	Push	6.00	8.00	3.77	6.72	-0.17	1.75	0.49	0.97	1.05	1.87	1.18	-0.48
4	K	20K	250	Up	PO	Dashed	Pull	6.10	7.50	3.77	1.94	-0.43	-0.14	-0.09	0.73	0.45	-5.67	0.17	1.25
4	K	20K	250	Up	PO	Dashed	Push	7.40	8.50	3.77	1.84	5.93	1.04	0.66	1.72	0.05	6.11	1.07	0.29
4	K	20K	250	Up	PO	Dashed	Pull	8.40	9.70	3.77	1.67	-1.46	-0.38	-0.43	0.58	0.30	-5.31	-0.25	1.03
1	M	20K	375	Up	PO	Solid	Push	1.50	3.00	4.712	6.54	-0.77	1.08	0.38	1.36	0.55	0.70	1.03	-0.64
6	H	20K	375	Up	PU	Dashed	Pull	3.00	4.80	3.59	3.41	0.54	1.16	0.29	1.66	0.60	-0.73	1.28	0.36
4	K	20K	375	Up	PO	Dashed	Push	3.00	6.00	5.834	2.78	-0.94	1.01	0.47	0.41	1.90	2.61	0.52	-0.33
6	H	20K	375	Up	PU	Dashed	Push	4.80	6.60	3.59	2.10	-1.04	1.97	0.81	0.63	0.50	2.16	2.05	-1.01
1	M	20K	375	Up	PO	Solid	Push	5.80	6.80	4.712	10.27	-2.41	0.96	2.72	0.82	0.35	7.30	1.48	-1.57
1	M	20K	375	Up	PU	Solid	Push	7.40	8.60	3.77	1.89	1.01	3.60	4.60	0.46	0.75	7.83	1.42	-5.76

#	P	Alt ft	A/S KIAS	Gear	Event	Bound	Motion	t _{start} sec	t _{end} sec	̇̇ _{pilot} rad/sec	Min Gain Time-to-Boundary				Max Gain Time-to-Boundary				
											t _{min} sec	K deg	G G	(ΔG/Δt) G/sec	t _{max} sec	Δt sec	K _{lim} deg	G G	(ΔG/Δt) G/sec
4	K	20K	375	Up	PO	Dashed	Push	7.80	8.60	5.834	2.25	2.31	1.30	6.32	0.39	0.25	7.20	2.04	-1.90
1	M	20K	375	Up	PU	Solid	Pull	8.50	9.90	3.77	2.40	-1.49	-0.17	-2.54	0.56	0.35	-1.58	0.70	4.82
4	K	20K	375	Up	PO	Dashed	Push	9.00	11.00	5.834	2.24	-1.88	0.97	-1.60	0.24	0.80	3.67	0.17	-1.54
4	K	20K	375	Up	PO	Dashed	Pull	10.50	12.00	5.834	1.79	1.63	-0.47	-0.12	1.18	0.15	-2.72	-0.43	0.57

Bibliography

- Brown, Frank and others. Flying Qualities Testing. Air Force Flight Test Center, Edwards AFB CA, 20 February 2002.
- Department of Defense. Flying Qualities of Piloted Aircraft. MIL-HDBK-1797. Washington: GPO, 19 December 1997.
- Gray, William. "Boundary-Escape Tracking: A New Conception of Hazardous PIO." Society of Experimental Test Pilots, 2004.
- Gray, William. "Boundary-Avoidance Tracking: A New Pilot Tracking Model." American Institute of Aeronautics and Astronautics, 2005.
- Matlab[®] /Simulink[®]. Version 2006a. Computer software. The Mathworks, Inc., Natick MA, 2006.
- McRuer, Duane T. "Pilot-Induced Oscillations and Human Dynamic Behavior." NASA-CR-4683, 1995.
- Mitchell, David G. and Roger H. Hoh. "Development of a Unified Method to Predict Tendencies for Pilot-Induced Oscillations." WL-TR-95-3049. Air Force Research Laboratories, Wright- Patterson AFB OH, June 1995.
- Preston, Jeff D. and others. "Unified Pilot-Induced Oscillation Theory, Volume 2: Pilot-Induced Oscillation Criteria Applied to Several McDonnell Douglas Aircraft." WL-TR-96-3029. Air Force Research Laboratories, Wright-Patterson AFB OH, December 1995 (ADB212157).
- Prosser, Kevin E. and others. "The Development of Nuisance Warning Criteria for Ground Collision Avoidance Systems: Preliminary Findings." Society of Experimental Test Pilots, 2001.

Vita

Randy Warren obtained his Bachelor of Science in Aerospace Engineering from the College of Engineering at the University of Tennessee (UT) in Knoxville, Tennessee. During his time at UT, he was selected for the NASA Academy summer research program at NASA's Goddard Space Flight Center; led the first UT team to conduct microgravity research on NASA's Weightless Wonder KC-135; served as the cadet wing commander for AFROTC Detachment 800; and helped design a human-powered lunar rover during an annual competition at NASA's Marshall Space Flight Center.

His military career began in 1992 when he enlisted in the Air Force as a Russian linguist. Upon his selection for the Airman Scholarship and Commissioning Program, he was discharged from active duty and began his studies at UT in 1997. He returned to service after being commissioned through AFROTC in 2001. He was assigned to Detachment 12 of the Space and Missile Systems Center in Albuquerque, NM. There he conducted mission operations for research and development satellite and space launch programs. He was selected for the joint AFIT-Test Pilot School Program in 2004 and is a graduate of USAF Test Pilot School Class 05B.

REPORT DOCUMENTATION PAGE			Form Approved OMB No. 074-0188		
The public reporting burden for this collection of information is estimated to average 1 hour per response, including the time for reviewing instructions, searching existing data sources, gathering and maintaining the data needed, and completing and reviewing the collection of information. Send comments regarding this burden estimate or any other aspect of the collection of information, including suggestions for reducing this burden to Department of Defense, Washington Headquarters Services, Directorate for Information Operations and Reports (0704-0188), 1215 Jefferson Davis Highway, Suite 1204, Arlington, VA 22202-4302. Respondents should be aware that notwithstanding any other provision of law, no person shall be subject to a penalty for failing to comply with a collection of information if it does not display a currently valid OMB control number. PLEASE DO NOT RETURN YOUR FORM TO THE ABOVE ADDRESS.					
1. REPORT DATE (DD-MM-YYYY) Dec 2006		2. REPORT TYPE Master's Thesis		3. DATES COVERED (From - To) Mar 2005 - Sep 2006	
4. TITLE AND SUBTITLE AN INVESTIGATION OF THE EFFECTS OF BOUNDARY AVOIDANCE ON PILOT TRACKING			5a. CONTRACT NUMBER		
			5b. GRANT NUMBER		
			5c. PROGRAM ELEMENT NUMBER		
6. AUTHOR(S) Warren, Randy D., Captain, USAF			5d. PROJECT NUMBER		
			5e. TASK NUMBER		
			5f. WORK UNIT NUMBER		
7. PERFORMING ORGANIZATION NAMES(S) AND ADDRESS(S) Air Force Institute of Technology Graduate School of Engineering and Management (AFIT/EN) 2950 Hobson Way, Building 640 WPAFB OH 45433-8865			8. PERFORMING ORGANIZATION REPORT NUMBER AFIT/GAE/ENY/06-S11		
9. SPONSORING/MONITORING AGENCY NAME(S) AND ADDRESS(ES) USAF Test Pilot School ATTN: Mr. William Gray III 220 S. Wolfe Ave. Edwards AFB, CA 93523 DSN 527-3000			10. SPONSOR/MONITOR'S ACRONYM(S)		
			11. SPONSOR/MONITOR'S REPORT NUMBER(S)		
12. DISTRIBUTION/AVAILABILITY STATEMENT APPROVED FOR PUBLIC RELEASE; DISTRIBUTION UNLIMITED.					
13. SUPPLEMENTARY NOTES					
14. ABSTRACT Pilot-Involved Oscillations (PIOs) remain a significant issue in the design, testing and operations of aerospace vehicles. Traditional methods for predicting, describing, and analyzing these events have provided the community with improved methods for minimizing the occurrences of PIOs. However, these events continue to occur over a wide range of aerospace vehicle types and over a wide range of pilot acumen. The introduction of boundary avoidance tracking (BAT) by Mr. William Gray in 2005 added a missing piece to the PIO puzzle. This theory presented that PIOs may result from increasing pilot gain resulting not from maintaining a specified condition, but avoiding imposed limits or boundaries on a specified task. The initial modeling and simulation conducted by Mr. Gray has provided the community with a starting point for applying this theory to the analysis of PIO events. This thesis characterizes BAT in the dynamic flight environment. Through the analysis of repeated BAT events in a T-38C aircraft, initial characteristic parameters for BAT have been identified and developed. The key BAT parameters were found to be independent of pilot and exhibited some dependence on aircraft load factor. Overall, BAT was successfully demonstrated and characterized during this research and the results will provide the community with a better understanding of the role BAT plays in PIO prediction and analysis.					
15. SUBJECT TERMS Pilot-involved oscillation, pilot-induced oscillation, T-38, T-38C, boundary avoidance tracking, flight test, Test Pilot School, TPS, HAVE BAT					
16. SECURITY CLASSIFICATION OF:			17. LIMITATION OF ABSTRACT	18. NUMBER OF PAGES	19a. NAME OF RESPONSIBLE PERSON
a. REPORT	b. ABSTRACT	c. THIS PAGE			19b. TELEPHONE NUMBER (Include area code)
U	U	U	UU	104	Paul A. Blue, Maj, USAF (937) 255-6565, ext 4714 (paul.blue@afit.edu)